Characterizing PD-L1-targeting extracellular vesicles produced by oncolytic Vaccinia virus infection

Submitted by: Ashley Chen

Supervisors: Dr. John Bell and Dr. Carolina Ilkow

Thesis submitted to the University of Ottawa in partial fulfillment of the requirements for the degree of Master of Science

Department of Biochemistry, Microbiology and Immunology

University of Ottawa
Faculty of Medicine
Ottawa, Ontario, Canada

Abstract

Tumour cells evade immune responses by multiple mechanisms in the tumour microenvironment, including through the expression of immunosuppressive molecules. The programmed cell death ligand 1 (PD-L1) plays a major role in this immunosuppression, and its expression is often up regulated as a result of innate and adaptive resistance mechanisms. Recent studies have discovered that the expression of PD-L1 can also extend to the nanoparticles that are naturally released by these cells, termed extracellular vesicles (EVs). Immune checkpoint inhibitors (ICIs) have shown great promise in blocking these immune-silencing interactions, but they remain hindered by their low response rates and toxic side effects. In addition, it has been found that the presentation of PD-L1 by EVs can be resistant to these established ICI therapies, further limiting their success. Here, we report a novel technique in which the oncolytic virus, Vaccinia virus, can be engineered to produce PDL1-targeting EVs as a form of immune checkpoint blockade. Our results show that our tailored EVs can target and neutralize immunosuppressive PD-L1, leading to enhanced anti-tumour immunity. Overall, this demonstrates the potential of using this technique to generate future EV-based immunotherapies.

Acknowledgements

I would like to thank my supervisor, Dr. John Bell, for giving me the opportunity to carry out my studies in his lab. With his support and guidance, I have been able to achieve my goals and develop into the young scientist I aspired to be. Throughout my time in the lab, I have also had the incredible privilege of working closely with Dr. Carolina Ilkow, who never failed to be a source of positivity, innovation, and guidance. I am extremely fortunate to have had the chance to work alongside these distinguished researchers. To Julia Petryk, our extraordinary animal and lab technician: thank you for your continued support over the course of my thesis. To my esteemed colleagues in the Cancer Centre (especially to those who have contributed directly to my thesis), it was a pleasure to spend my days (and nights) with you all – your passion and determination continues to inspire me. Lastly, to my family and friends: without you, I could not have accomplished everything I have, and I am extremely fortunate to have such a strong support system.

List of Abbreviations

PD-L1 – programmed cell death ligand 1

EV – extracellular vesicles

ICI – immune checkpoint inhibitor

OV – oncolytic virus

TIME – tumour immune microenvironment

IFN – interferon

VacV – Vaccinia virus

CTLA-4 – cytotoxic T-lymphocyte-associated antigen-4

PD-1 – programmed cell death protein-1

WT – wild type

MOI – multiplicity of infection

pfu – plaque-forming unit

kb – kilobases

List of Figures

Table of Contents

1. Introduction

1.1 Oncolytic viruses (OVs) as anti-cancer therapies

1.1.1 Immunoresistance drives the need for novel therapies

Despite the continuing advancements made everyday in cancer research, new obstacles continue to emerge and challenge the field. A recent study suggests that approximately 1 in 2 Canadians is expected to be diagnosed with cancer at some point during their lifetime [1], suggesting the need for effective therapeutics is more prevalent than ever. Currently, it is standard for surgery and/or radiotherapy to be used in the treatment of localized tumours; however, it has become evident that many cancers are able to develop resistance to these, and other treatments [2,3]. This concept of resistance, including immune evasion and immunosuppression, represents one of the major challenges facing the field today. Through diverse mechanisms of innate and adaptive immune suppression, tumours act to prevent or restrain any effector T-cell responses[4–7]: these mechanisms often include, changing the antigen profile, to make the tumours less detectable by effector T-cells[8,9]; blocking T-cell recruitment to the tumour[10,11]; exploiting immunosuppressive leukocytes, such as regulatory T-cells and tumour-associated macrophages[12–14]; and even, producing molecules that can actively inhibit tumour-specific T-cells that enter the tumour immune microenvironment (TIME) [15,16]. In an effort to combat this resistance, treatment strategies that focus on stimulating and/or further boosting the anti-tumour immune response are being actively investigated. Immune checkpoint inhibitors (ICIs) [17], adoptive cell therapies[18], chimeric-antigen receptor T-cells[19], anti-cancer vaccines[20], and oncolytic viruses (OVs) [21] are examples of these immunotherapeutic strategies that have garnered increasing interest over the years.

1.1.1 Overview of OV potential

Oncolytic viruses (OVs) represent a promising immunotherapy based on their dual capacity to selectively infect and kill tumour cells, while inducing a systemic anti-tumour immune response[4]. Their selectivity stems from the observation that the anti-viral host machinery found in normal cells is often deficient in cancer cells[4,22]. For example, protein kinase R (PKR) aids in the clearance of intracellular viral infections; however, this factor is often absent in some cancer cells, allowing increased viral replication[21]. In addition, malignant defects in the type I interferon (IFN) signaling pathway have been associated with enhanced susceptibility to viral infection[23]. Therefore, many factors produced following infection – such as those involved in the inhibition of cell growth, activation of apoptosis, and stimulation of the immune response – are defective in cancer cells, making them more susceptible to viral infection[24]. This selectivity for malignant cells, with little to no harm to normal cells, makes OVs a promising therapeutic strategy, and they provide the specificity that conventional therapies (ex. chemotherapy) lack.

While viral-induced oncolysis was initially thought to be the major contributor to tumour clearance, increasing evidence suggests that the induction of a sufficient anti-tumour immune response is also essential for complete eradication of the tumour[25]. An example of this was seen where the OV-mediated anti-tumour activity was eliminated following targeted T-cell disruption before intratumoural injection of oncolytic adenovirus. Despite the fact that OV replication and persistence was significantly increased in their absence, the combination effect with the immune cells was needed for efficient tumour clearance[26]. This suggests that these OV-induced immune stimulation events, while being in some capacity anti-viral (thereby potentially restricting viral replication and spread to some degree), are essential to

the anti-tumour immune response[27,28]. This concept has been supported by the success of the oncolytic Herpes simplex virus type I (HSV-1), Talimogen Laherparepvec (T-VEC) [29,30], and the oncolytic vaccinia virus, pexastimogene devacirepvec (Pexa-Vec) [31]. These two OVs have been engineered to express the granulocyte macrophage colony-stimulating factor (GM-CSF), based on its immune-stimulating ability to promote antigen-presenting cell (APC) recruitment and maturation, demonstrating the synergy of OVs with immune functions[30]. Therefore, it is likely that the most effective treatment regiment for OV therapy will be one in which potent viral oncolysis is combined with an effective and durable anti-tumour immune response[4].

1.2 Vaccinia virus (VacV)

1.2.1 VacV as an OV platform

One well-characterized and frequently used OV platform is Vaccinia virus (VacV). It belongs to the *Poxviridae* family, and is characterized by a single, double-stranded, linear DNA genome[32,33]. From each infected cell, VacV can produce four different types of virion: the intracellular mature virus (IMV), the intracellular enveloped virus (IEV), the cell-associated enveloped virus (CEV), and the extracellular enveloped virus (EEV) [33]. The IMV form of VacV is the most abundant, and is recovered following cell lysis when performing viral purification[32,34]. For this thesis, the Copenhagen (Cop) wild-type strain of Vaccinia was used as the OV platform. This choice was made based on preliminary studies done by our group, in which Copenhagen was found to replicate better than the other tested Vaccinia strains (Tian Tan, Wyeth, Western Reserve, and Lister) in the cancer cells and tumour samples tested (Pelin *et al;* manuscript in preparation).

VacV demonstrates many advantages as an OV over other viral candidates, including: 1- its extensive clinical experience in humans for smallpox vaccinations; 2- its large transgene encoding capacity; 3- its broad cell tropism; and, 4- its unique life cycle that occurs solely in the cytoplasm [21,32,34–38]. The enhanced transgene encoding capacity is owing to the characteristic large genome of VacV that is around 190 kb in length[39]. It has even been observed that the genome can accommodate an additional 25 kb of foreign DNA sequence[40,41], further demonstrating that the VacV platform is ideal for the incorporation of numerous therapeutic transgenes that can target various stages of the cancer-immunity cycle. Another characteristic that is unique to VacV is its ability to infect and replicate in a wide range of host cells[32,34]. This facilitates the transition of experiments from *in vitro* to *in vivo* models, and also provides a more accurate interpretation of findings that can be expected from the clinic. However, despite its wide host range, VacV still exhibits a natural tropism for tumour cells[32]. For example, it was shown that a few days following intravenous (IV) injection, the greatest amount of virus was found in the tumour, with minimal to no virus recovered from other organs. This finding was consistent across several tumour models, including murine colon cancer and melanoma, rat sarcoma, human colon cancer in nude mice, and rabbit kidney cancer[34,42–45]. The life cycle of VacV and other poxviruses is also quite unique in that it exists solely in the cytoplasm, as there is no integration of foreign or recombinant DNA into the host genome[34,37]. Instead, it is observed that host protein synthesis is completely halted by 4-6 hours post-infection, allowing for efficient expression of viral genes and replication, solely by virally-encoded enzymes[32,34,38]. Therefore, VacV is largely able to evade host detection, minimizing the risk of unwanted OV-induced anti-viral immunostimulation, as mentioned above.

1.2.2 Current obstacles and opportunities for improvement

While VacV serves as an optimal platform for OV therapies, it does still face certain limitations. For example, despite its large cloning capacity, it has been observed that the expression of cytokines from VacV can slightly hinder the replication and oncolytic potential of the virus[46]. It is likely that this is related to the fact that using cytokines to boost the immune response can also lead to unwanted anti-viral effects, therefore limiting viral spread and replication within the host. An ideal situation would be one in which OV infection stimulates the immune response, but there is a delay in the occurrence of anti-viral activity. Therefore, viral persistence is limited only once the OV-induced anti-tumour immunity has been sufficiently established. Another major hurdle for OV therapy, especially in terms of translating VacV therapy to the clinical landscape, is the ability to enhance viral delivery to tumour sites. It is important to note that this limitation exists for other OV platforms as well, and is not exclusive to poxviruses. Based on data from clinical trials, the traditional intravenous route of injection is well-tolerated with limited toxicity; however, the efficacy has been below expectations[47]. It is likely that prior to reaching the TIME, the injected free virions are encountering several hurdles following injection, such as neutralizing antibodies, complement activation, anti-viral cytokines, tissue-resident macrophages, and/or non-specific uptake by other tissues (ex. lung, liver and spleen) [47,48]. Based on some preliminary studies, it has been shown that the intratumoural (IT) delivery route can be safely used in humans[49], but is limited to easily reachable solid tumours, and is considerably more invasive for the patient[47]. Therefore, VacV therapies will benefit from techniques that enhance their targeting specificity for the TIME. This thesis focuses on developing a novel strategy that will assist in tackling this issue.

1.3 The evolution of immune checkpoint inhibitor (ICI) therapies

1.3.1 Overview of ICIs and their targets

As mentioned previously, one of the immunotherapies that has demonstrated significant success in combating the innate and adaptive immunosuppression observed in the TIME are immune checkpoint inhibitors, or ICIs. Many checkpoint receptors that play a role in regulating T-cell function to prevent autoimmunity have been identified (see Fig 1.1)[50]. As a form of immune resistance, tumour cells are able to exploit these naturally occurring, immune-regulating mechanisms for their own benefit. This has led to the development of ICIs, or antibodies that function to block these immune-silencing interactions from occurring, thereby leading to enhanced anti-tumour immunity downstream. Cytotoxic T-lymphocyte-associated antigen-4 (CTLA-4; also known as CD152) was the first checkpoint receptor to be clinically targeted based on its function in suppressing the activity of the T-cell co-stimulatory receptor, CD28, during initial stages of T-cell activation[51–53]. Monoclonal antibodies targeting CTLA-4 demonstrated success in blocking these immunosuppressive activities and enhancing the anti-tumour immune response[7,54,55], which lead to their Food and Drug Administration (FDA) approval and transition to clinical use[50].

The success with CTLA-4 paved the way for researching additional immune checkpoint targets, such as the programmed cell death protein-1 (PD-1; also known as CD279). PD-1 is a surface receptor that, contrary to CTLA-4, is only expressed once the T-cells become activated[56]. It has also been identified on activated B-cells, dendritic cells, monocytes, and natural killer cells[57–60]. The two ligands for PD-1 are PD-1 ligand-1 (PD-L1; also known as B7-H1 and CD274) and PD-1 ligand-2 (PD-L2; also known as B7-DC and CD273) [61–64]. Upon engagement of PD-L1 with PD-1, there is subsequent dephosphorylation

of the co-stimulatory receptor, CD28, and the T-cell receptor (TCR), leading to T-cell suppression[65]. It has been well characterized that through both innate[66,67] and adaptive[68–70] immune resistance mechanisms, some tumour cells exhibit up regulated expression of PD-L1, contributing to the immunosuppression seen in the TIME[50]. This has led to the investigation (and now clinical use) of monoclonal antibodies targeting the PD-1/PD-L1 axis based on their ability to combat these immunosuppressive functions and reactivate the CD28 signaling pathway, thereby enhancing anti-tumour T-cell activity[71,72].

1.3.2 Current limitations restricting their success

While ICI antibodies targeting CTLA-4 and PD-1 have shown great promise as effective immune-stimulating therapies, they are not without their limitations. For example, clinical studies using CTLA-4 antibodies have reported a high frequency of immune-related toxicities[50]. This finding is not surprising, however, since it was demonstrated in *Ctla4*-knockout mice that this deletion results in lethal systemic immune hyperactivation, due to the key role that CTLA-4 plays in regulating T-cell activation[73,74]. Fortunately, it appears that ICI treatments targeting PD-1 are substantially less immunotoxic than anti-CTLA-4, since it was found that only 1 of 39 patients had a severe immune-related adverse event during the initial Phase I trial of anti-PD1 therapy[50]. This is consistent with the findings in mice where *Pd-1* deletion led to autoimmune disease as well, but it developed later in life and was less severe than the *Ctla-4* deletion[75,76]. Therefore, this provides a rationale for further investigating anti-PD-1/PD-L1 therapies in the context of this project.

Another limitation that has been identified for ICI therapies is the surprisingly low response rate. It has been reported that even the best response rates in initial clinical studies do not typically exceed 35% to 40% [36,77–85]. Unfortunately, multiple factors exist that could

be hindering the success of these ICI therapies, especially amongst different tumour models being tested. Some of these may include, the immune context of the TIME (ex. tumour models that exhibit a more immunologically "cold" TIME tend to be less responsive to ICIs[86,87]); the availability, immunogenicity, and frequency of tumour antigens; the pharmacodynamics and pharmacokinetics of the ICI, to ensure that it can be efficiently delivered and distributed throughout the TIME; and the overall expression of the target immune checkpoint protein[7,88]. While additional research needs to be done to better understand these ICIs and their functionality across different cancer models, these findings do support the notion that instead of giving the ICIs as a monotherapy, they may show the best success when administered as a combination therapy with additional immune-stimulating strategies. This should then enable ICIs to have a better response rate across a wider range of tumour models and a larger number of patients.

1.3.3 Rational combination of ICIs with OV therapies

Recent studies have prioritized investigating combination strategies with ICIs that will facilitate re-modeling of the TIME, such that it is more immunogenic and sensitive to the immunotherapy[86,87,89,90]. As mentioned previously, OVs are gaining recognition for their ability to additionally induce a systemic anti-tumour immune response[4]. This provides rationale for combining OVs with ICIs, such that the OVs can assist in generating a more immunogenic TIME that will enhance the efficacy of ICI treatment, thereby overcoming the immunosuppression that may in turn be hindering the oncolytic potential of the OVs[91]. Examples[92] can already be seen in which ICIs were successfully combined *in trans*, as individual treatments, with OVs[77,93], or *in cis*, as an engineered transgene to encourage localized delivery and expression within the TIME[94–98].

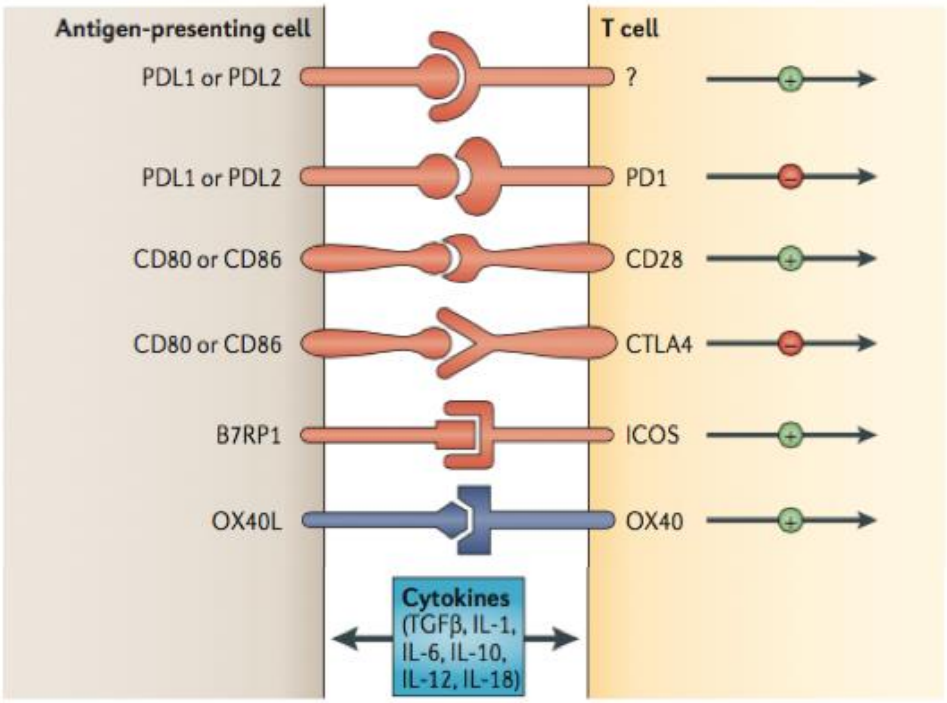

Figure 1.1 Co-stimulatory and inhibitory interactions for regulating T-cell responses. This figure has been adapted from Pardoll[50]. Depicted are a few of the known co-stimulatory and inhibitory interactions that can occur between an antigen-presenting cell, and the T-cell, to regulate T-cell responses. Inhibitory interactions primarily function to prevent auto-immunity. ICIs currently being tested in the clinic target CTLA-4 and the PD-L1/PD-1 axis.

1.4 Extracellular vesicles (EVs) as an immunotherapeutic platform

1.4.1 Growing interest in the EV field

One area of interest that has gained significant momentum over the past decade in understanding the biological basis of cancer and other diseases is the study of extracellular vesicles (EVs). In the past nine years, results for EV publications have increased 733-fold – mirroring a similar trajectory to what was observed in the past for the study of T-cell subsets, circulating B-lymphocytes, and circulating tumour cells[99]. Classified as endogenous nanoparticles that are naturally released by both eukaryotic and prokaryotic cells[100,101], EVs can be subdivided into three main classes: exosomes, microvesicles, and apoptotic bodies[102,103]. Exosomes, usually ranging in size from 30 to 150 nm in diameter, are derived from the endolysosomal pathways. They are formed within multivesicular bodies (MVBs), and released by cells upon fusion of the MVBs with the plasma membrane[104]. Microvesicles differ in their mode of release, as they form following direct outward budding of the plasma membrane. Therefore, they tend to be larger than exosomes, falling anywhere within the 50 to 1000 nm diameter size range[105]. Apoptotic bodies are formed, as the name suggests, during apoptosis and the rearrangement of the cytoskeleton, then released through outward blebbing and decomposition of the cell membrane[105]. Their size range is the largest, ranging from 500 to 2000 nm in diameter[106].

EVs have demonstrated the ability to transfer their biological content – consisting of proteins, lipids, and nucleic acids – to facilitate their role in cell-to-cell communication[106–111]. Therefore, they have garnered major interest for therapeutic applications, including but not limited to: as biomarkers for disease, based on the fact that they carry genetic information and molecular signatures from their originating, parent cells[102,103]; and, as drug delivery

systems, since they possess signal molecules to facilitate their intrinsic capacity to target cells of interest[112–116]. There is no denying that as researchers continue to study and better understand these EVs, it will generate a wealth of opportunities for possible applications in novel therapies.

1.4.2 Newly identified key contributors of immunosuppression

While the intrinsic function to facilitate cell-to-cell communication by EVs, or more particularly by exosomes, has proven advantageous for some preliminary therapies, there has also been substantial evidence to suggest a malignant role of exosomes in cancer development. In particular, exosomes have been implicated in the formation of the pre-metastatic tumour nice, to generate an immunosuppressive TIME[100,117–120]. For example, exosomes were shown to transfer functional EGFRvIII protein amongst cancer cells in a glioblastoma model, aiding in the transformation of wild-type cells and propagating their cell growth[108]. In melanoma, exosomes were found to drive lung metastases formation by transferring the oncoprotein, MET, to bone marrow progenitor cells[118].

In the context of this project, it has also been found that cancer-derived exosomes can transfer and express PD-L1, inhibiting immune responses in the TIME, and contributing to increased tumour burden[121–123]. In fact, the removal of exosomal PD-L1 expression, either by genetically blocking exosome biogenesis or by deleting *Pd-l1*, was able to reverse the malignant phenotype, promoting effector T-cell functions and sensitizing tumour models to ICI therapies[123]. There was also a strong correlation found between patients with a higher level of circulating exosomal PD-L1 before anti-PD1 treatment, and poorer clinical outcomes. This highlights a key role that exosomal PD-L1 expression plays in contributing to

the immunosuppression of the TIME, and therefore its potential as a predictive biomarker for PD-1 therapy resistance[121,122,124].

1.4.3 The successful tailoring of EVs for therapeutic strategies

While the field of EVs still has many unanswered questions, this has not prevented researchers from discovering successful strategies to engineer these nanoparticles for therapeutic use. In particular, the ability to engineer tailored exosomes for targeted therapies has been of interest to this project. In the original study by Alvarez-Erviti *et al.*[125], it was discovered that a targeting peptide of interest (ex. rabies viral glycoprotein; RVG) could be fused to the extra-exosomal N-terminus of Lamp2b, a protein found abundantly in exosomal membranes[126]. This enabled safe and specific delivery of IV-injected exosomes to neurons, microglia, and oligodendrocytes in the brain[125]. Following this study, Ohno *et al.* fused the GE11 peptide to the transmembrane domain of the exosomal platelet-derived growth factor receptor protein; this enabled efficient delivery of the tailored exosomes to epithelial growth factor receptor (EGFR)-expressing breast cancer cells[127]. Koh *et al.* found that exosomes expressing a SIRP-α variant not only targeted CD47 on cancer cells as expected, the exosomes were also able to function as an ICI. This enabled blocking of the CD47/SIRP-α interaction, leading to an enhanced anti-tumour immune response and improved tumour control[128]. It is important to note that in the study, a comparison of the exosomal presentation of the SIRP-α variant versus administration of the SIRP-α variant as a monomer (similar to traditional therapies) was performed. The results showed that exosomal presentation of the ICI was significantly better at improving tumour control, thereby providing support for the tailoring of EVs as an ICI delivery platform, rather than the traditional antibody delivery[128].

1.4.4 Potential application of EV strategies for novel therapies

The application of exosomes as delivery systems has garnered major interest over recent years, largely due to their intrinsic targeting abilities, and their capacity to carry biological information[112–116]. It has also become evident that these exosomes possess additional advantages over some nanoparticle technologies currently being used. For example, since exosomes are endogenous signaling nanoparticles, they have better biocompatibility and stability; and are therefore less immunogenic, non-cytotoxic, and non-mutagenic, compared to other existing foreign delivery vehicles. These attributes become especially pertinent when repeat dosing is required for treatment[100,127–129]. In addition, their cellular origin enables exosomes to overcome naturally existing barriers, which has been demonstrated with their infiltration of the blood-brain barrier[100,125]. Overall, these naturally derived exosomes serve as a promising alternative vector to overcome some of the obstacles hindering current therapeutic success.

Another application for engineered EV strategies to consider is their use to target the immunosuppressive exosomes produced in some tumour models. As mentioned previously, exosomal PD-L1 expression has been identified as a key contributor of immunosuppression in the TIME[121,122,124], and data gathered by Poggio *et al.* suggest that this exosomal PD-L1 is resistant to traditional anti-PDL1 therapy[123]. This was demonstrated in the TRAMP-C2 prostate cancer model, which is known to be resistant to anti-PDL1 antibodies, when following removal of exosomal PD-L1, mice were sensitized to checkpoint therapy and tumour growth was inhibited[123]. The origin of this exosomal resistance remains unclear, however it is possible that it could be related to, how the PD-L1 is being expressed on exosomes, the magnitude of exosomal expression, and/or the ability of exosomes to reach

targets that are sequestered from the effects of the antibody[123]. Therefore, it is likely that a technique in which exosomes can be engineered to target and neutralize immunosuppressive PD-L1-expressing exosomes will be more effective than traditional ICI antibody-based therapies, improving the anti-tumour immune response. This thesis focuses on possible strategies to apply this concept.

1.5 Project Rationale

One of the major challenges limiting the success of cancer research is immune resistance. Through both innate and adaptive resistance mechanisms, tumours act to prevent or restrain effector T-cell responses in the TIME. ICIs have demonstrated success in certain cancer models, but remain hindered by this immunosuppression. This suggests the potential for combination treatments of ICIs with other immune-stimulating therapies. OVs serve as ideal immunotherapy platforms for this combination based on their tumour cell selectivity, capacity for engineered transgene expression, and their ability to enhance anti-tumour immunity. Endogenous nanoparticles, termed exosomes, expressing PD-L1 have been identified as key contributors of immunosuppression in the TIME. Unfortunately, traditional ICI antibodies do not efficiently target these exosomes, suggesting the need for alternative approaches.

In this thesis, we investigate the possibility of engineering EVs expressing PD-1 to function as an ICI, thereby allowing the targeting and neutralizing of immunosuppressive PD-L1 expression in the TIME. For this, we propose engineering an oncolytic VacV to produce these tailored EVs, such that the therapy can be 1) easily delivered as a monotherapy; 2) more economical, since the OV will be used to produce the EVs, rather than requiring direct administration of the EVs (used in current treatments); and 3) more concentrated in the TIME, based on the tumour selectivity of the OV platform.

1.6 Hypothesis

The oncolytic Vaccinia virus can be engineered to produce extracellular vesicles targeting PD-L1 for immune checkpoint blockade.

1.7 Experimental Objectives

1. Demonstrate that VacV infection leads to increased EV marker expression.
2. Engineer the Copenhagen Wild-type strain of VacV to produce tumour-targeting EVs, as a proof-of-concept.
3. Validate that the PD-1 targeting peptide allows the EVs to bind PD-L1.
4. Confirm that immune checkpoint blockade by PD-1 EV presentation enhances anti-tumour immunity.

2. Materials and Methods

2.1 Cell lines and culture

All cell lines were purchased from the American Type Culture Collections (Manassas, VA), except those that were gifted (CT26-mPDL1-KO, CT26-mPDL1-KO + Thy1.1-mPDL1) from the laboratory of Dr. Michele Ardolino (University of Ottawa). Mammalian cells were cultured in Dulbecco's modified Eagle's medium (DMEM) (Corning cellgro, Manassas, VA) or RPMI-1640 (CT26-WT, CT26-mPDL1-KO, CT26-mPDL1-KO + Thy1.1-mPDL1) (Corning cellgro, Manassas, VA) supplemented with 10% fetal bovine serum (FBS) (HyClone, GE Healthcare Bio-sciences, Pittsburgh, PA) and maintained at 37°C with 5% CO_2. Cells were routinely tested for mycoplasma contamination using the e-myco VALID Mycoplasma PCR Detection Kit (Cat# 25239, FroggaBio, Toronto, ON, Canada) and Hoechst staining[130].

2.2 DNA constructs and viral constructs

The Exo-PD1 construct had to be generated from two separate gBlock® Gene Fragments (Integrated DNA Technologies, Coralville, IA), due to the fragment size restrictions. The B14R-KO control construct was obtained by using a primer that replaces the mPD-1 gene of the first gBlock with a FLAG tag: GACTACAAAGACGAT-GACGACAAG. The two fragments for each virus were designed to include compatible XhoI restriction sites, such that the digested gBlocks could be ligated together using T4 DNA ligase (M0202S, New England Biolabs, Ipswich, MA). The constructs were then inserted into the B14R locus of the Copenhagen strain of Vaccinia virus, as previously described[131,132]. The sequences of the primers used for recombination into the B14R locus were as follows: forward: AATATTAATATTAGACTATCTCTATCGCG ;

reverse: AGTGCACAAGTTGCTGCAG

2.3 Virus quantification and viral kinetics assay

Viral titers and assessment of viral kinetics were obtained by plaque assays. For testing the kinetics, different viral constructs were used to infect U2OS cells seeded as monolayers in 6-well plates at a multiplicity of infection (MOI) of 0.1. The plates were then stored in the -80°C freezer at the corresponding time-points (i.e. 0, 24, 48, 72 hours post-infection), and thawed immediately prior to titering. Serial dilutions of the samples were prepared in serum-free DMEM. The dilutions were then transferred to monolayers of U2OS cells –seeded the day before – and incubated at 37°C for 2 hours. After the incubation, cells were overlayed with 3% Carboxymethylcellulose (CMC) in DMEM supplemented with 10% FBS. Plates were incubated for 48 hours at 37°C with 5% CO_2, then the plaques were counted following crystal violet staining. Viral titers are quantified as number of plaque forming units/mL (PFU/mL).

2.4 Virus rescue and purification

Virus rescues were performed as previously described[131,132]. U2OS cells were infected with the Copenhagen strain of vaccinia virus (CopWT) at an MOI of 0.05. Following a 2-hour incubation, the media was removed and cells were transfected with the viral construct DNA, facilitated by the Lipofectamine 2000 reagent (Thermoscientific, Waltham, MA), and left overnight at 37°C with 5% CO_2. The media was then replaced with fresh DMEM supplemented with 10% FBS, and left for an additional 24-48 hours at 37°C with 5% CO_2, or until a good CPE was observed. At that point, the plate was freeze-thawed using a -80°C freezer, and the supernatant was used to infect U2OS cells.

For expansion and purification of the recombinant viral preparations, confluent U2OS or HeLa cells were infected at an MOI of 0.02 for approximately 72 hours at 37°C, or until a sufficient CPE was observed. At this point, the entire media and cell mixture was collected, and spun at 3000 rpm for 10 minutes to pellet the cells. The supernatant was discarded, and the infected cells were resuspended in 1mM Tris pH 9.0, and underwent three freeze-thaw cycles using the -80°C freezer to ensure sufficient lysis of the cells. The suspension was then centrifuged at 2500 rpm for 5 minutes, and the supernatant (cleared lysate) was applied to a 36% sucrose cushion for additional centrifugation at 12,500 rpm for 1h30 at 4°C. The resulting viral pellet was resuspended in Formulation buffer, and this viral stock was stored at -80°C or 4°C short-term.

2.5 EV purification/isolation

When isolating small EVs, a minimum of two 15cm dishes was used per condition. Cells were plated, and once they reached 90-100% confluency, they were infected at an MOI of 1 or 10, and left at 37°C with 5% CO_2 for 2 hours. The media was then completely removed and replaced with DMEM supplemented with 10% exosome-depleted FBS. After 48 hour incubation at 37°C with 5% CO_2, the supernatant was collected and spun sequentially at 1000g for 10 minutes, 2000g for 20 minutes, 12,000g for 30 minutes, and 120,000g for 3 hours – refrigerated at 4°C the entire time. The resulting pellet was then resuspended in 35 mM Trehalose for long-term storage at -80°C.

2.6 Western Blots and Immunoprecipitation (IP) Pull-down Assay

Cell pellets or EVs were lysed on ice for 20-30 minutes using complete protease inhibitor cocktail (Roche, Mississauga, ON, Canada) in RIPA lysis and extraction buffer (Cat# 89901, Thermoscientific, Waltham, MA), then centrifuged for 15 minutes at 12,000

rpm. Prior to loading the samples for Western Blot analysis, they were often normalized using the Pierce BCA Protein Assay Kit (23225, Thermoscientific, Waltham, MA).

For the immunoprecipitation (IP) pull-down assay, isolated EVs were diluted in Dulbecco's phosphate-buffered saline (Corning Cellgro, Manassas, VA) and rotated overnight at 4°C with 12ug/mL of CD279 (PD-1) antibody (Clone J43) (Cat# 14-9985-82, eBioscience, Life Technologies, Carlsbad, CA). The following day, the recombinant protein G sepharose beads (Cat# 101241, Life Technologies, Carlsbad, CA) were spun at 500g for 5 minutes, and washed in PBS 3 times. The beads were then added to the EV samples, and rotated for 2-3 hours at 4°C to allow binding; after which, the bead-EV complexes were spun at 500g for 5 minutes, and washed 2 times with PBS.

All samples were mixed with dithiothreitol-supplemented loading buffer (250 mM Tris- HCl pH 6.8, 10% SDS, 30% glycerol, 5% DTT, 0.02% bromophenol blue). The samples were migrated on Bio-Rad Mini Protean 4-15% TGX Protein Gels (Bio-Rad, Mississauga, ON, Canada) and transferred onto PVDF membranes (Bio-Rad, Mississauga, ON, Canada), prior to blocking with 5% skim milk powder (Sigma-Aldrich, St. Louis, MO) in tris-buffered saline (TBS) with 0.1% Tween-20 (P9416, Sigma-Aldrich, St. Louis, MO). The membranes were then probed using the following antibodies: mouse anti-Alix (ab117600), mouse anti-Calreticulin (ab22683), rabbit anti-Vaccinia virus (A27L; ab35219), rabbit anti-mouse PD-1 (ab214421), mouse anti-HA tag (ab25631), rabbit anti-mouse PD-L1 (ab213480), rabbit anti-CD9 (ab92726) (Abcam, Cambridge, UK); goat anti-TSG101 (sc6037; Santa Cruz, Dallas, TX); mouse anti-Flotillin-1 (610821; BD Biosciences, San Jose, CA); rabbit anti-GM130 (12480), rabbit anti-Tom20 (42406), rabbit anti-β-actin (4970S), rabbit anti-GAPDH (2118) (Cell Signaling Technology, Danvers, MA). The membranes

were then probed with horseradish peroxidase-coupled anti-rabbit (7074S) or anti-mouse (7076S) secondaries (Cell Signaling Technology, Danvers, MA), and then imaged using Clarity Max Western ECL Reagent (Cat# 1705062) and a ChemiDoc Imaging System (Bio-Rad, Mississauga, ON, Canada).

2.7 Nanoparticle Tracking Analysis (NTA)

Isolated EVs for NTA were diluted in PBS and analyzed on the ZetaView® ParticleMetrix video microscope. Experimental parameters for camera control usually included a sensitivity of 80, a frame rate of 30, and a shutter speed of 70.

2.8 ELISA: mPD-1 and Binding Set-ups

The concentration of mPD-1 in mock or virus-infected supernatant samples was determined using the mouse PD-1 ELISA kit (ab217609, Abcam, Cambridge, UK) according to the manufacturer's protocol; to ensure no signal resulted from the virus, the supernatant was subjected to a 0.22μm filter to filter out any VacV particles. Additional components used were the recommended Nunc MaxiSorp 96-well Immunoplate (Cat# 430341, Thermoscientific, Waltham, MA), Coating Buffer (ab210899), TMB ELISA Substrate (High Sensitivity; ab171523), and the 450nm Stop Solution for TMB Substrate (ab171529).

For the Binding ELISA set-up, the Capture antibody from the mouse PD-1 ELISA kit (ab217609, Abcam, Cambridge, UK) was used at the recommended 2ug/mL concentration in Coating Buffer, and left to coat overnight at 4°C with gentle shaking. The plates were then treated with Blocking Buffer (1% BSA, 0.05% Tween® 20, in 1X PBS, pH 7.2 - 7.4) for 2 hours at room temperature with shaking to reduce non-specific binding, followed by mock or virus-infected lysate sample addition at the indicated total input protein concentrations based on the BCA Protein Assay kit. This was left overnight at 4°C with gentle shaking. On the

third day, 4ug/mL of mPD-L1-Biotin (Cat# 71119, BPS Biosciences, San Diego, CA) in Blocking Buffer was added for 2 hours at room temperature with shaking to allow binding with the mPD-1 present in the samples. HRP-Streptavidin (ab210901, Abcam, Cambridge, UK) was then added at 0.05ug/mL in Blocking Buffer for 1 hour at room temperature with shaking, until 20 minutes of treatment with the TMB Substrate, and addition of the 450nm Stop Solution prior to plate reading. All fluorescence/absorbance readings were taken at 450nm or 570nm wavelength using a Multiskan Ascent (Thermo Labsystems, Beverly, MA).

2.9 Quantitative PCR (qPCR)

For activation qPCR analysis, 12-wells were pre-coated with 1ug/mL anti-CD3e (Cat# 550275) and 2ug/mL anti-CD28 (Cat# 553295) (BD Biosciences, San Jose, CA) overnight at 4°C. T-cells were isolated using the EasySep Mouse T-cell Isolation Kit (Cat# 19851, StemCell Technologies, Vancouver, BC, Canada) from Balb/c spleens, and added at a concentration of 3.5e6 cells/well in complete RPMI media (10% heat-inactivated FBS, 1% Pen-Strep, 1% L-glutamine, and 50uM β-mercaptoethanol) to activate overnight at 37°C with 5% CO_2. The next day, 80ug of EVs (determined by BCA Protein Assay) were added to the T-cells for each condition, and left for 48 hours at 37°C with 5% CO_2. After which, the RNA was extracted using TRIzol reagent (Life Technologies, Carlsbad, CA) according to the manufacturer's protocol. The RNA concentration and purity was assessed using a NanoDrop ND-1000 spectrophotometer (Thermoscientific, Waltham, MA) prior to reverse transcription using iScript cDNA Synthesis Kit (Bio-Rad, Mississauga, ON, Canada). mRNA qPCR primer sequences were[133]: 18S rRNA_For: GTAACCCGTTGAACCCCATT, 18S rRNA_Rev: CCATCCAATCGGTAGTAGCG, mIL-2_For: TTGTG-CTCCTTGTCAACAGC, mIL-2_Rev: CTGGGGAGTTTCAGGTTCCT, mIFN-

γ_For: TTCTTCAGCAACAGCAAGGC, mIFN-γ_Rev: TCAGCAGCGACT-CCTTTTCC, mIL-4_For: AACGAGGTCACAGGAGAAGG, mIL-4_Rev: TCTGCAGCTCCATGAGAACA, mTNF-α_For: ATGAGCACAGAAAGCATGA, mTNF- α_Rev: AGTAGACAGAAGAGCGTGGT, mIL-12_For: GATG-ACATGGTGAAGACGGC, mIL-12_Rev: AGGCACAGGGTCATCATCAA, mTGF-β_For: CCTGCAAGACCATCGACATG, mTGF-β_Rev: TGT-TGTACAAAGCGAGCACC. For the qPCR, PerfeCTa SYBR Green FastMix (95072-012, Quantabio, Beverly, MA) was used according to manufacturer's protocol, and the samples were analyzed using an SDS 7500 Fast Real-time PCR Machine (Applied Biosystems, Foster City, CA). 18S rRNA was used as the endogenous housekeeping control for all samples. To calculate ΔΔCt, the average 18S rRNA Ct from mock samples was subtracted from the Ct value for the target of interest in the same mock samples (control delta). The Ct values for 18S rRNA from the experimental samples were subtracted from the Ct value for the target of interest in the same experimental samples (experimental delta). Control delta was subtracted from experimental delta and the resulting ΔΔCt value was input into the formula 2^-ΔΔCt to obtain a final ΔΔCt value.

2.10 Flow cytometry and CFSE EV Transfers

For analysis of mPD-L1 expression, CT26-WT, CT26-mPDL1-KO, and CT26-mPDL1-KO + Thy1.1-mPDL1 cells were seeded at 5e5 cells/mL in 6-wells of RPMI-1640 + 10% FBS, and left overnight at 37°C with 5% CO_2. The next day, cells were either mock-treated or treated with 50U/well of Recombinant Mouse IFN-γ Protein (485-MI-100, R&D Systems, Minneapolis, MN), and left overnight at 37°C with 5% CO_2. At 24 hours post-treatment, the infected and mock-infected cells were washed with PBS, trypsinized, and spun

at 1500 rpm for 5 minutes to remove the supernatant. The cell pellets were then resuspended in PBS, and added to a V-bottom 96-well plate for staining. A 1:20 dilution (in PBS) of BV510 Fixable Viability Stain RUO (564406, BD Biosciences, San Jose, CA) was used for all wells, except the unstained controls, and left for 20min at room temperature in the dark. After which, the plate was centrifuged at 1500rpm for 5min, and the supernatant was removed. A 1:100 (in PBS) dilution of the CD274 (B7-H1; mPD-L1) Monoclonal (MIH5), SuperBright780 (78-5982-82, eBioscience, Life Technologies, Carlsbad, CA), or its isotype control – Rat IgG2a kappa Isotype Control (eBR2a), SuperBright780 (78-4321-80, eBioscience, Life Technologies, Carlsbad, CA) – was added to the corresponding wells, and left for 20min at room temperature in the dark. The plate was then centrifuged at 1500rpm for 5min, the supernatant was removed, and the cells were fixed with 200uL of 4% paraformaldehyde (PFA).

For the Carboxyfluorescein succinimidyl ester (CFSE) EV transfer experiments, small EVs were isolated using the protocol outlined above (**2.5 Small EV purification/isolation**), and the input amounts were normalized using the Pierce BCA Protein Assay Kit. The EV pellets were then stained with an equal volume of 80uM CFSE (65-0850-84, eBioscience, Life Technologies, Carlsbad, CA) for 1 hour at room temperature in the dark. For removal of excess reagent, the EVs were resuspended in PBS and centrifuged again overnight at 120,000g, refrigerated at 4°C. CT26-WT, CT26-mPDL1-KO, CT26-mPDL1-KO + Thy1.1-mPDL1 were seeded at 3e5 cells/mL. The next day, the purified CFSE-labeled EVs were collected in PBS, and used to treat each cell line for 2 hours at 37°C with 5% CO_2. Following this incubation, the cells were washed with PBS, trypsinized, and spun at 1500rpm for 5min. The resulting cell pellet was resuspended and fixed with 4% PFA

for subsequent analysis by flow cytometry. This CFSE staining and treatment protocol has been adapted based on one developed by Chen *et al*[121].

When performing flow cytometry, samples fixed in 4% PFA would be diluted, as needed, in FACS buffer (PBS + 5% fetal calf serum). All samples were analyzed using either the BD LSRFortessa, or the BD FACSCelesta flow cytometers. The gating strategy used for all samples was performed as described (see Fig 2.1).

2.11 Quantification and Statistical Analysis

Differences between groups were calculated using two-way ANOVA when more than one independent variable was included, followed by the Bonferroni's post-test. When only one independent variable was tested for the qPCR assay, a one-way ANOVA was used with Tukey's multiple comparison test. Data was processed with GraphPad Prism, Version 5 (GraphPad Software). In all cases a P value of 0.05 and below was considered significant: $p < 0.05$ (*), $p < 0.01$ (**), and $p < 0.001$ (***). Details regarding number of replicates can be found in the legends.

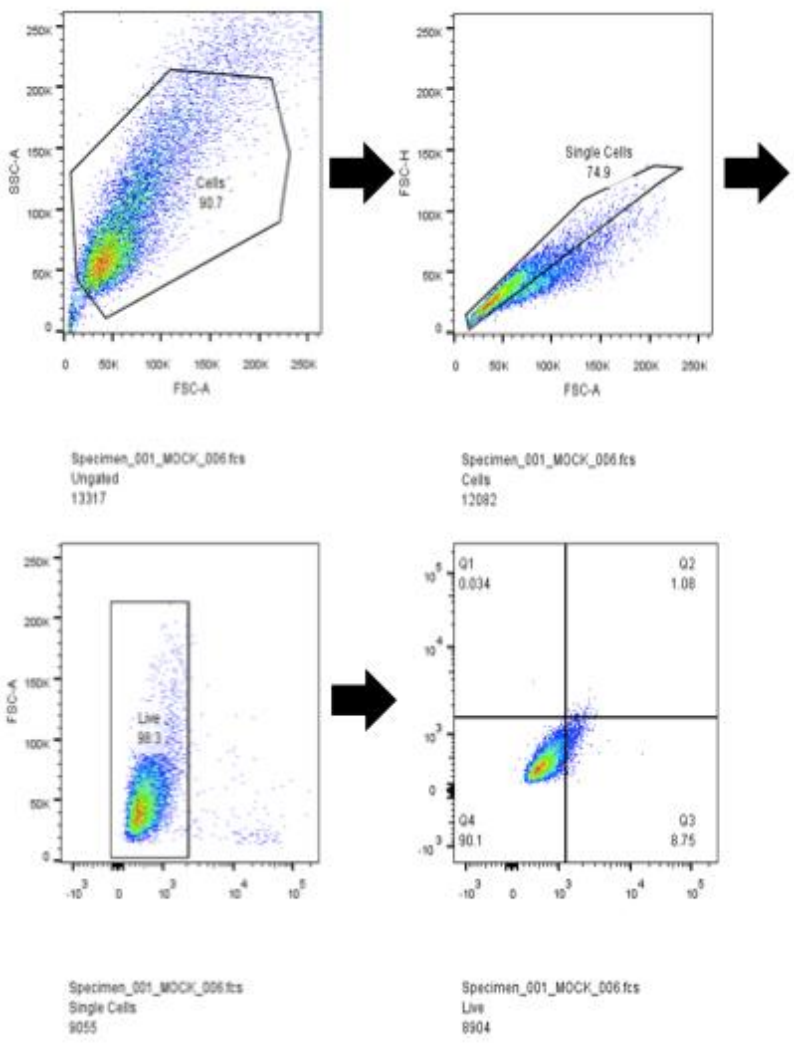

Figure 2.1 Gating strategy used for analysis of single, live cells by flow cytometry. For analysis of all samples by flow cytometry, the following gating strategy was used. This was done to ensure that all results represented expression by live cells, rather than non-specific staining due to cellular debris and/or other artifacts in the samples. The strategy includes first gating on cells, based on forward scatter and side scatter (first panel); then gating on single cells, based on forward scatter alone (second panel), to emit analysis of doublets and/or other groups of cells; and finally, gating on cells that do not emit signal following staining with the viability dye (third panel), since cells that do label and are bound by the dye are dead. Once this gating process was complete for all samples (fourth panel), the analysis for targets of interest could be performed.

3. Results

3.1 VacV infection enhances EV expression in multiple cancer cell lines

To demonstrate the first objective, EVs were collected from human cancer cell lines (Vero, 786-0, and HT-29) following mock infection, or infection with the Copenhagen Wild-type (CopWT) strain of VacV at an MOI of 1 for 48 hours. Western blot analysis was done on the isolated purified EVs, and their corresponding whole cell lysates (WCL; Fig 3.1). Increased EV expression following VacV infection was confirmed by probing for characteristic EV protein markers, including: ALG-2-interacting protein X (Alix), the tumour susceptibility gene 101 protein (TSG101), and Flotillin-1, which are involved in sorting cargo into exosomes, and are associated with the endosomal sorting complex required for transport (ESCRT)[106,134,135]. To validate that the isolated EV fractions were pure and did not contain cellular content, they were probed for cellular markers, including: GM130 (Golgi Apparatus), Calreticulin (endoplasmic reticulum; ER), and Tom20 (Mitochondria)[136]. The originating whole cell lysates (WCLs) were probed with the same markers and on the same membranes to serve as positive controls. An antibody targeted to the A27L protein of VacV was used to serve as validation of VacV infection in the correct conditions, and to confirm that the EV purification method successfully filters out all VacV. This method is based on an optimized separation protocol that has been developed and used in our lab.

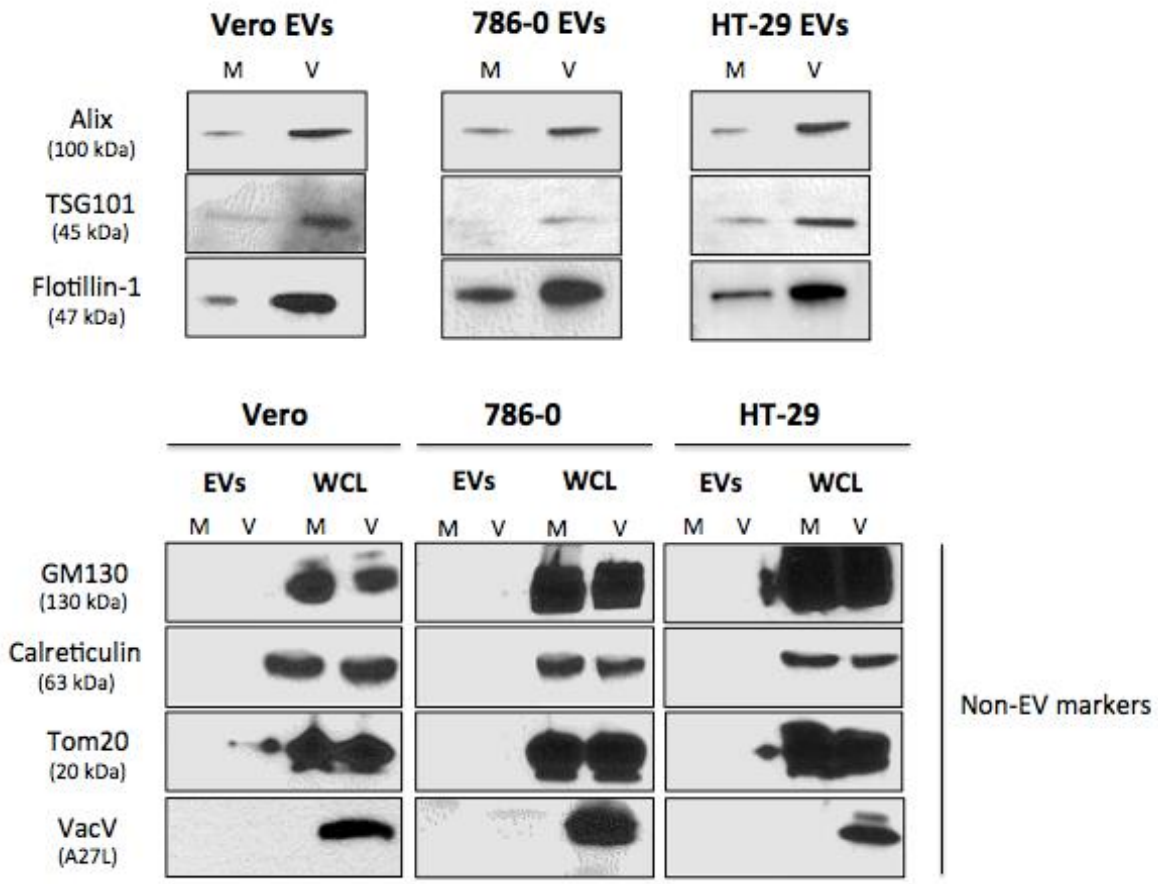

Figure 3.1 VacV infection leads to increased EV marker expression. Western blot analysis of EVs and WCLs from Vero, 786-0, and HT-29 cells following mock infection (M), or CopWT infection (V) at an MOI of 1, 48 hours post-infection (hpi). The membranes were probed for EV markers (Alix, TSG101, and Flotillin-1), cellular/non-EV markers (GM130, Calreticulin, Tom20), and the A27L protein of VacV.

3.2 CopWT can be engineered to produce tumour-targeting EVs

Since it has been previously demonstrated that exosomes, or EVs, can be engineered to display a targeting peptide of interest[125,127,128], we sought to determine if CopWT can be used to produce EVs expressing a tailored peptide. As a proof-of-concept, the mouse version of PD-1 (mPD-1) was chosen as the targeting peptide, and the FLAG tag was used as a control peptide. These targeting peptides were fused to the exosomal membrane protein, lamp2b[125,126]. The mouse version of PD-1 was used to allow future *in vivo* testing, for targeting mouse PD-L1. These constructs were inserted into the B14R locus of CopWT (Fig 3.2A) and mCherry-positive plaques indicated successful generation of the recombinant viruses; fluorescence microscopy was used for detection of these plaques (Fig 3.2B). From this point forward, the resulting recombinant viruses will be referred to as VacV-Exo-PD1 (in which mPD-1 is the targeting peptide), and VacV-B14R-KO (in which the FLAG tag is the targeting peptide control).

In order to ensure that expression of these tailored exosome constructs did not significantly alter the replication and growth kinetics of the VacV-Exo-PD1 and VacV-B14R-KO recombinant viruses, a time course of the viral titers was performed 0, 24, and 48 hpi using U2OS cancer cells. The viral titers were compared to an equivalent CopWT virus, in which the B14R locus was interrupted with the mCherry fluorescent protein sequence alone (named Cop-B14R-RFP; Fig 3.3B). Visual validation of infection was confirmed by fluorescence microscopy (Fig 3.3A), and this fluorescence signal was used during isolation of the recombinant viruses.

To confirm transgene expression of mPD-1, 786-0 cells were infected at an MOI of 1 for 48h, and a portion of the supernatant was collected for analysis by sandwich ELISA (Fig

3.4A); the corresponding WCLs were collected, and the remaining supernatant was used to isolate EV fractions for Western Blot analysis (Fig 3.4B). For the sandwich ELISA, the samples for each condition were first subjected to BCA analysis to determine the protein concentration. Based on this analysis, known total input protein concentrations were used for each condition in the ELISA. The results show significant, concentration-dependent expression of mPD-1 following VacV-Exo-PD1 infection, which is absent in the mock infected and control virus (VacV-B14R-KO) conditions. Probing for the EV marker, Alix, was done to confirm that the EV fraction was loaded for each condition. In addition, the results are consistent with increased EV marker expression following VacV infection, as seen in Fig 3.1.

Once the concentration-dependent expression of mPD-1 was confirmed, we sought to verify that the Exo-PD1 chimera exhibits the correct membrane topology, thus enabling the targeting abilities of the tailored EVs to PD-L1. To this end, I performed an immunoprecipitation (IP) pull-down assay (Fig 3.5A). For this assay, EVs were collected from CT26-lacZ mock-infected cells, or cells that had been infected at an MOI of 1 for 48h with either the VacV-B14R-KO control virus, or the VacV-Exo-PD1 virus. The purified EVs (resuspended in PBS) were incubated with an anti-mPD-1 antibody, or with a negative control anti-IgG antibody, overnight with rotation. The following day, an equal volume of Sepharose beads were added to each sample, and incubated for 2-3 hours. After, the bead-EV complexes were spun down and subjected to Western Blot analysis (Fig 3.5B). The results obtained from these experiments show that only EVs produced following VacV-Exo-PD1 virus infection could be bound by the anti-mPD-1 antibody, collected by the Sepharose beads, and detected by Western blot analysis. This was done by probing for the EV markers,

Alix and Flotillin-1, since EVs should only be collected by the Sepharose beads and detected by Western blot when they exhibit the correct Exo-PD1 chimera on their membrane surface. This signal is also lost when the EVs from the same VacV-Exo-PD1 virus condition are incubated with the negative control, anti-IgG antibody, suggesting that the pull-down is specific for the anti-mPD-1 antibody, and dependent on its binding with the mPD-1 targeting peptide of the Exo-PD1 chimera. This suggests that the Exo-PD1 chimera is being displayed correctly on the EV membrane surface following VacV-Exo-PD1 infection, as depicted in Fig 3.5C. Expression of the heavy chains of the antibodies due to cross-reactivity for each condition was used as a loading control. The originating WCLs were also probed for Alix and Flotillin-1 expression on the same membrane as a positive control.

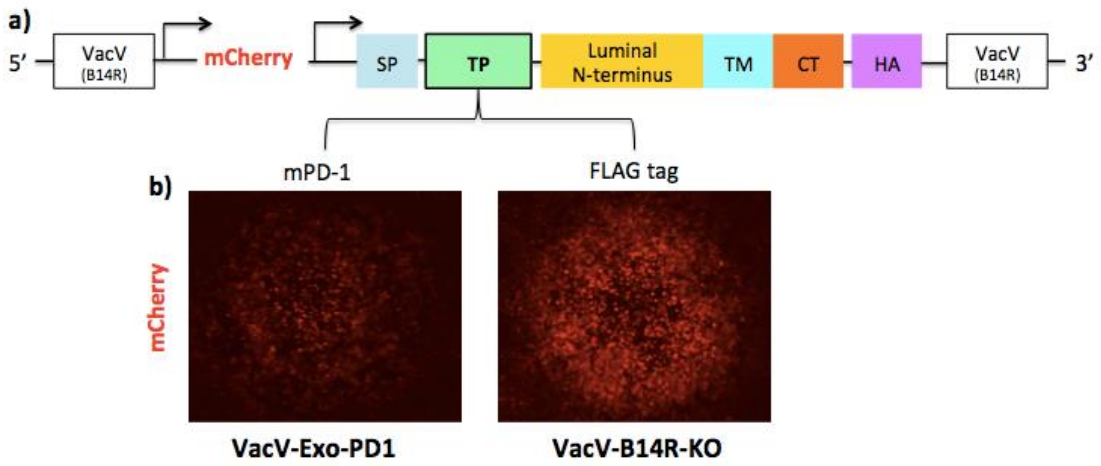

Figure 3.2 CopWT can be engineered to express the Exo-PD1 construct. (A) Schematic representation of the recombinant viral construct inserted into the B14R locus of the CopWT strain of Vaccinia virus; SP, signaling peptide; TP, targeting peptide; luminal N-terminus, transmembrane, and cytosolic domain of exosomal membrane protein, lamp2b; HA, human influenza hemagglutinin tag. (B) Fluorescence microscopy images of mCherry-positive plaques with recombinant viruses VacV-Exo-PD1 (TP: mPD-1), and VacV-B14R-KO control (TP: FLAG tag) in U2OS cells.

a)

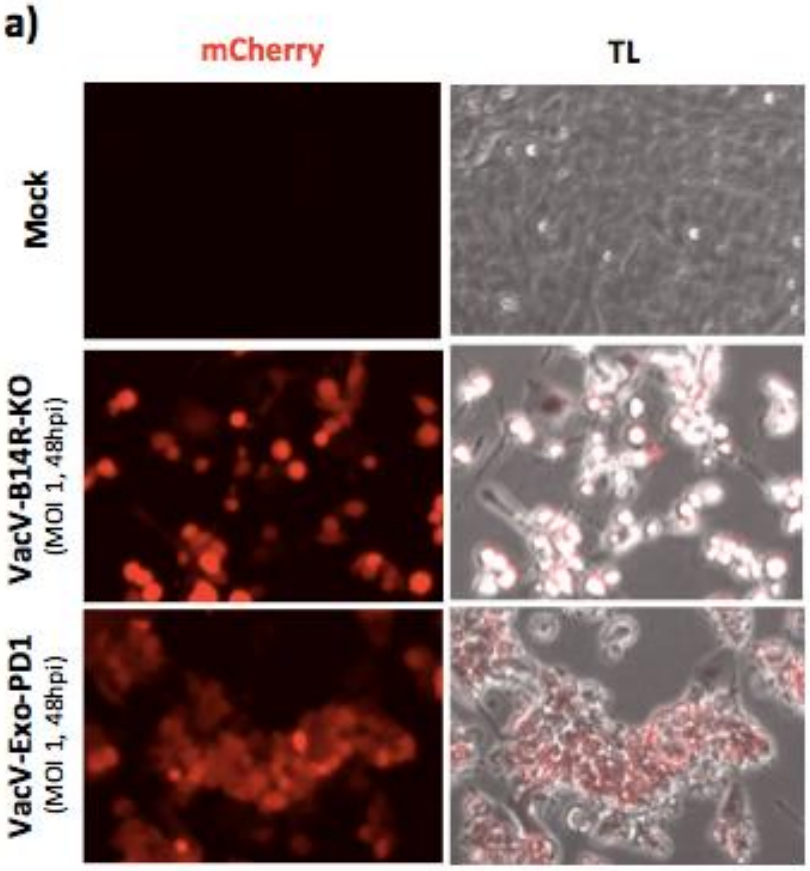
mCherry
TL
Mock
VacV-B14R-KO
(MOI 1, 48hpi)
VacV-Exo-PD1
(MOI 1, 48hpi)

b)

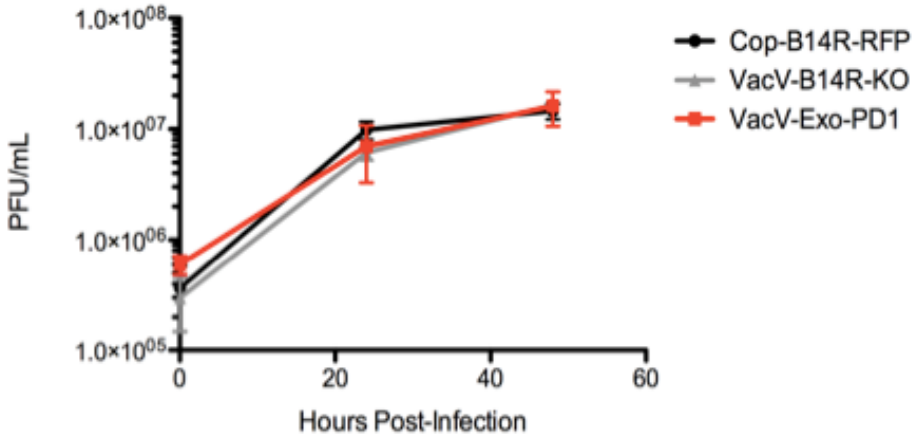
1.0×10^08
1.0×10^07
1.0×10^06
1.0×10^05
PFU/mL
0
20
40
60
Hours Post-Infection
Cop-B14R-RFP
VacV-B14R-KO
VacV-Exo-PD1

Figure 3.3 Infection and replication is not significantly altered for the recombinant viruses. (A) Fluorescence microscopy images of mCherry/RFP expression following mock, VacV-B14R-KO control, or VacV-Exo-PD1 infection at an MOI of 1 for 48h. TL, transmitted light. (B) Time course of viral titers (in PFU/mL) from U2OS cells infected at an MOI of 0.1 for 0h, 24h, and 48h, with Cop-B14R-RFP (mCherry only), VacV-B14R-KO (TP: FLAG tag), or VacV-Exo-PD1 (TP: mPD-1). No statistical significance was observed at all time-points (two-way ANOVA, Bonferroni's post-test).

a)

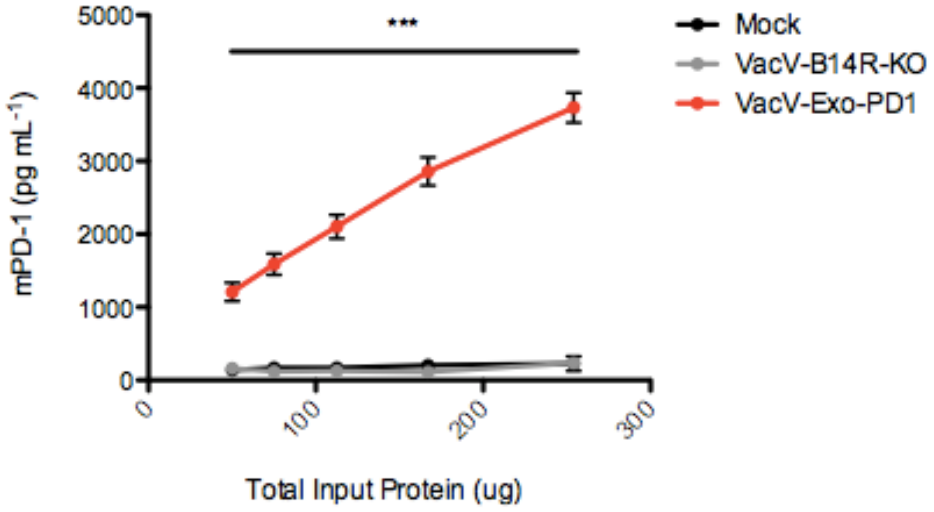
***
Mock
VacV-B14R-KO
VacV-Exo-PD1
mPD-1 (pg mL-1)
5000
4000
3000
2000
1000
0
0
100
200
300
Total Input Protein (ug)

b)

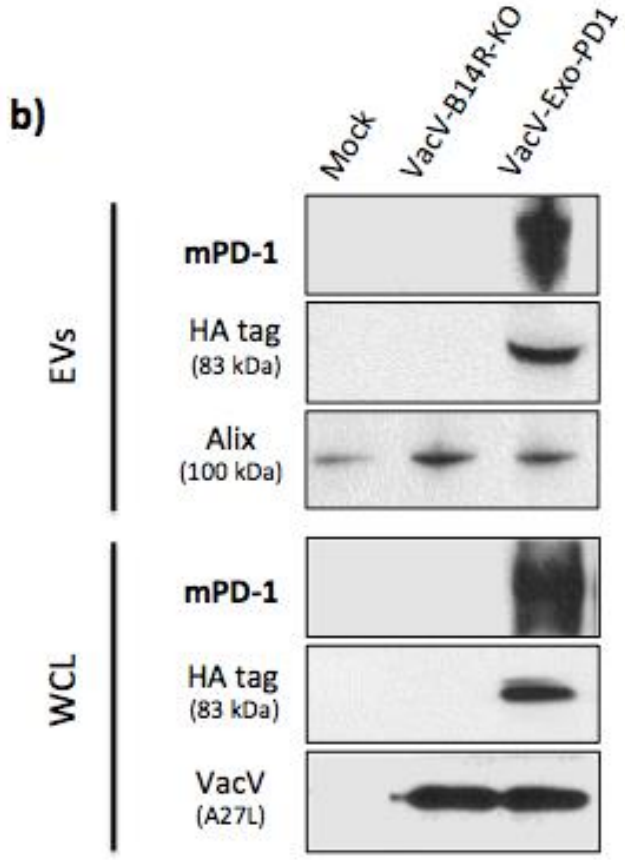
Mock
VacV-B14R-KO
VacV-Exo-PD1
EVs
mPD-1
HA tag
(83 kDa)
Alix
(100 kDa)
WCL
mPD-1
HA tag
(83 kDa)
VacV
(A27L)

Figure 3.4 Detection of mPD-1 expression following VacV-Exo-PD1 infection. (A) Sandwich ELISA for mPD-1 expression, as a measure of the total input protein (in μg) in the supernatant collected from 786-0 cells following mock-infection, or infection with VacV-B14R-KO control, or VacV-Exo-PD1 viruses at an MOI of 1 for 48h. Each data point represents 3 biological replicates, using the average of 2 technical replicates. The difference between mock-infection and VacV-Exo-PD1 infection was significant at all input protein concentrations: ***P<0.001, confirmed by two-way ANOVA and Bonferroni's post-test. The difference between the VacV-B14R-KO and the VacV-Exo-PD1 conditions was also significant at all input protein concentrations: ***P<0.001, confirmed by two-way ANOVA and Bonferroni's post-test. The difference between mock-infection and the VacV-B14R-KO infection conditions was not statistically significant. (B) Western blot analysis of the EV fractions and WCLs of 786-0 cells following mock-infection, or infection with VacV-B14R-KO control, or VacV-Exo-PD1 viruses at an MOI of 1 for 48h. The membranes were probed for mPD-1 and the HA tag (to confirm proper chimeric transgene expression), the EV marker Alix, and the A27L protein of VacV.

a)

1) anti-mPD1 is added to the EV sample

2) anti-mPD1 binds EVs expressing Exo-PD1 chimera

3) Sepharose beads bind the EV-ExoPD1 complex

4) Sepharose beads bound to EV-ExoPD1 are pulled down and collected for Western blot analysis

b)

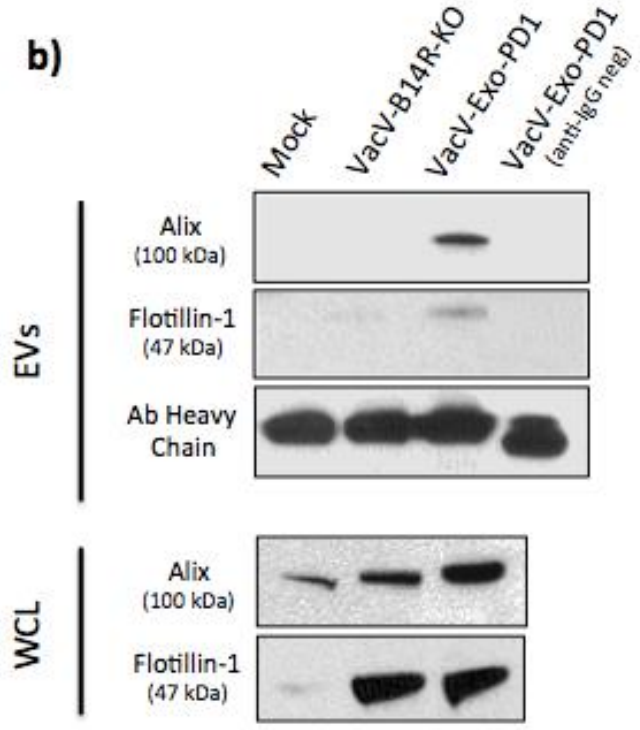

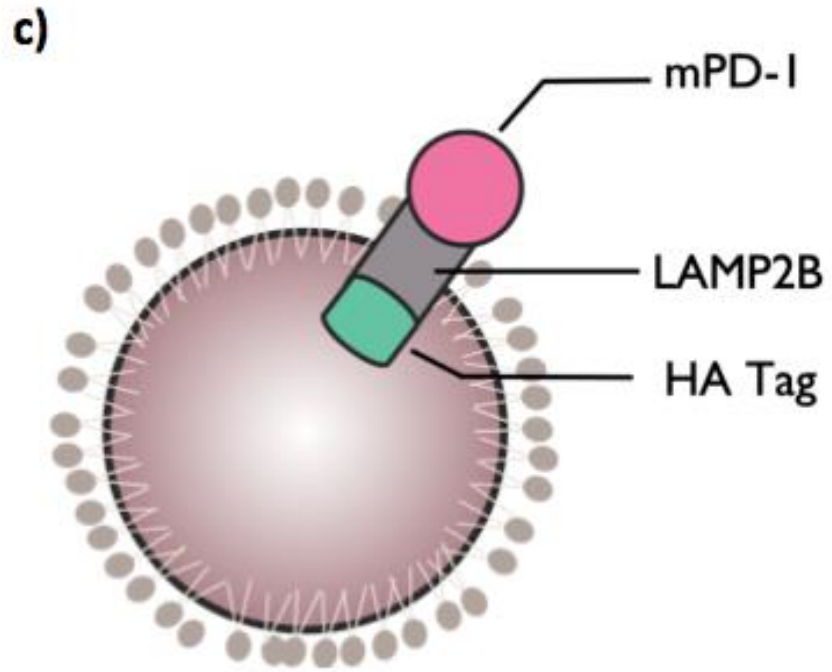

Figure 3.5 Exo-PD1 chimera on tailored EVs exhibits the correct membrane topology. (A) Schematic representation of the IP pull-down assay set-up[137]; an anti-mPD-1 (Clone J43) antibody or a negative control anti-IgG antibody was used with Sepharose beads. (B) Western blot analysis of the collected EV fractions following IP pull-down, and the originating WCLs. The EVs and WCLs were collected from CT26-lacZ cells that had been either mock infected, infected with the VacV-B14R-KO control virus, or infected with the VacV-Exo-PD1 virus at an MOI of 1 for 48h. The membranes were probed for EV markers, Alix and Flotillin-1, to detect any EVs expressing the Exo-PD1 chimera correctly, and had therefore been pulled down by the IP. Detection of the heavy chains of the antibodies due to cross-reactivity was used as a loading control for each condition. (C) Schematic representation of the Exo-PD1 chimera displayed by an EV, based on the design construct described in Fig 3.2.

3.3 mPD-1 displayed on tailored EVs preferentially binds mPD-L1

Based on the results observed in Section 3.2, the recombinant virus, VacV-Exo-PD1, produces EVs expressing the Exo-PD1 construct, as expected. Next, we sought to investigate whether the Exo-PD1 chimera can bind mPD-L1. For this, an initial assay was used based on a variation of a binding ELISA. In this experimental set-up, an mPD-L1 protein conjugated to biotin binds mPD-1 from the Exo-PD1 construct, resulting in fluorescence signal that can be quantified. Samples lacking mPD-1 expression (due to absence of the Exo-PD1 chimera) should therefore not bind the mPD-L1, resulting in little to no fluorescence signal. Schematic representation of this assay can be seen in Fig 3.6A. Lysates were collected 48hpi from CT26-WT cells following mock infection, or infection at an MOI of 10 (due to the reduced viral infectivity of this cell line) with the VacV-B14R-KO control virus, or the VacV-Exo-PD1 virus. For this binding ELISA, the samples for each condition were first subjected to BCA analysis to determine the protein concentration. Based on this analysis, known total input protein concentrations were used for each condition. For each virus treatment, an additional condition was included in which the lysates were pre-incubated with the anti-mPD-1 antibody for 2 hours prior to addition to the ELISA set-up. This pre-treatment was done to block the interaction between the mPD-1 (of the Exo-PD1 chimera) and mPD-L1, to ensure that any fluorescence observed was due to this interaction. Absorbance readings relative to the negative control (in order to discount background signal) demonstrate the greatest fluorescence signal for the VacV-Exo-PD1 condition, as expected (Fig 3.6B). It is also important to note that the fluorescence signal for the VacV-Exo-PD1 condition is lost when the lysates are pre-incubated with an anti-mPD-1 antibody; thus validating that the signal observed is due to mPD-1 binding to mPD-L1. This is further confirmed by the

observation that for the mock infected and VacV-B14R-KO control virus conditions (with and without anti-PD-1 antibody), there is little to no difference in absorbance.

While the binding ELISA is successful at confirming that cellular mPD-1 expression produced following VacV-Exo-PD1 infection binds to mPD-L1, it is unable to demonstrate that this binding is also observed for the tailored EVs produced following infection. For this, an additional assay was performed, based on one developed by Chen *et al*[121]. In this assay, EVs are isolated from 786-0 cells, stained with Carboxyfluorescein succinimidyl ester (CFSE) dye for 1 hour, and then transferred to recipient cells (Fig 3.7A). To better demonstrate that uptake of these fluorescently labeled EVs is affected by mPD-L1 expression, CT26 cells with varying mPD-L1 expression were used: CT26-WT, CT26-mPDL1-KO, and CT26-mPDL1-KO + Thy1.1-mPDL1. To confirm the differential mPD-L1 expression in each of these cell lines prior to carrying out the experiment, flow cytometry (Fig 3.7B) and Western blots were used (Fig 3.7C). In these validation experiments, conditions included mock treated cells versus cells collected after 24 hour treatment with 50U/well of Recombinant Mouse IFN-γ Protein, based on the well-characterized relationship of mPD-L1 up-regulation following IFN-γ treatment[50] (functioning here as a positive control for some conditions). As expected, the CT26-WT cells displayed moderately low levels of mPD-L1 for the mock condition, which was increased to almost 100% of the live cell population following IFN- γ treatment, based on flow cytometric analysis (Fig 3.7B). The CT26-mPDL1-KO cells exhibited no mPD-L1 expression for both conditions, and the CT26-mPDL1-KO + Thy1.1-mPDL1 displayed constant high levels of expression for both conditions, with 100% of the live cell population positive for mPD-L1.

Preliminary results for the CFSE EV transfer experiment demonstrate a positive shift in fluorescence intensity when EVs are collected following VacV-Exo-PD1 infection, and transferred to cells with the highest constant level of mPD-L1 expression (CT26-mPDL1-KO + Thy1.1-mPDL1) (Fig 3.8). This shift in intensity suggests that the recipient cells for this condition, compared to the others, are taking up more CFSE-labeled EVs displaying the Exo-PD1 chimera. These results were consistent with what was expected, since these CT26-mPDL1-KO + Thy1.1-mPDL1 cells exhibit the greatest level of mPD-L1 that could be targeted for uptake by the fluorescent mPD-1-expressing EVs, resulting in greater CFSE signal. It is important to note that prior to transferring the EVs from each virus condition to the recipient cells, they were subjected to BCA analysis in an attempt to normalize the concentration of EVs used for each condition. For each recipient cell-type, the fluorescence intensity of CFSE remained relatively constant for the condition in which EVs were collected from 786-0 cells following infection with the VacV-B14R-KO control virus. These results were expected based on the lack of a compatible targeting peptide for these EVs. It is also reassuring to know that these preliminary results reflect those observed by Chen *et al*, when they used a similar experimental set-up[121].

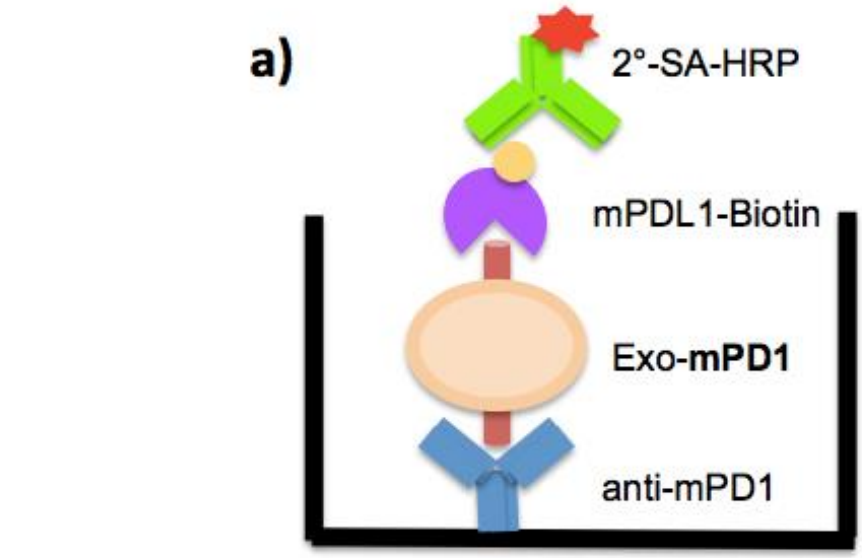
a)
2°-SA-HRP
mPDL1-Biotin
Exo-mPD1
anti-mPD1

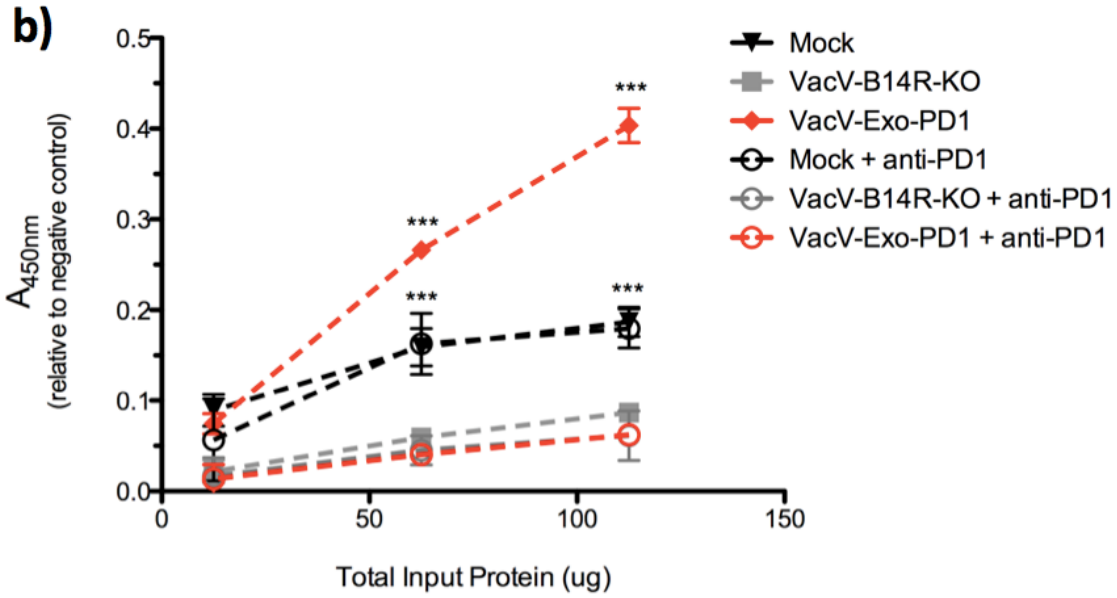
b)
A450nm
(relative to negative control)
0.5
0.4
0.3
0.2
0.1
0.0
0
50
100
150
Total Input Protein (ug)
***
***
***
***
Mock
VacV-B14R-KO
VacV-Exo-PD1
Mock + anti-PD1
VacV-B14R-KO + anti-PD1
VacV-Exo-PD1 + anti-PD1

Figure 3.6 Exo-PD1 produced by recombinant VacV-Exo-PD1 infection binds mPD-L1. (A) Schematic representation of the binding ELISA set-up: SA- Streptavidin; HRP- horseradish peroxidase. (B) Absorbance readings at 450nm for each condition, relative to the negative control (to discount background signal), were plotted as a function of the total input protein (in μg) in the CT26-WT cell lysate samples. Conditions included mock-infection, following VacV-B14R-KO control infection, or following VacV-Exo-PD1 infection at an MOI of 10 for 48 hours. Additional conditions were included in which the cell lysate samples were pre-incubated for 2 hours with an anti-mPD-1 antibody. Each data point represents 4 biological replicates, using the average of 2 technical replicates. Statistical significance was confirmed using a two-way ANOVA and Bonferroni's post-test: ***P<0.001.

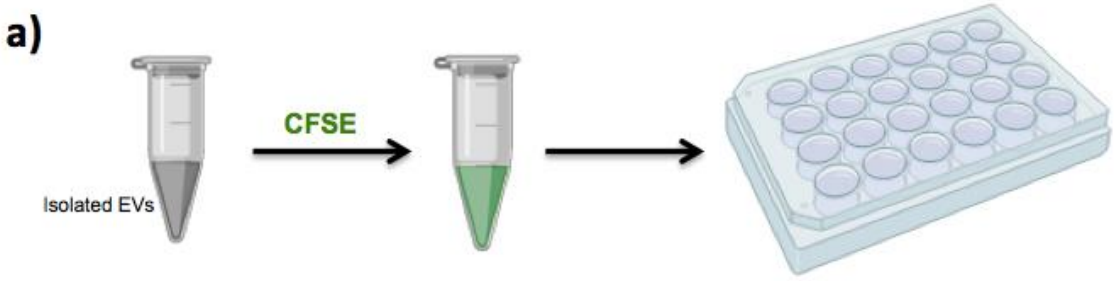
a)
CFSE
Isolated EVs

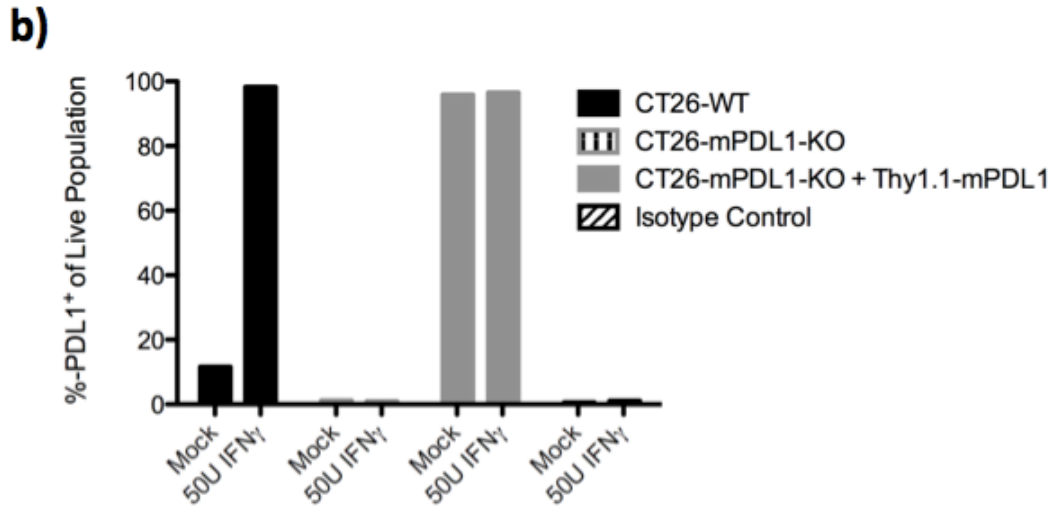
b)
%-PDL1+ of Live Population
100
80
60
40
20
0
Mock
50U IFNγ
Mock
50U IFNγ
Mock
50U IFNγ
Mock
50U IFNγ
CT26-WT
CT26-mPDL1-KO
CT26-mPDL1-KO + Thy1.1-mPDL1
Isotype Control

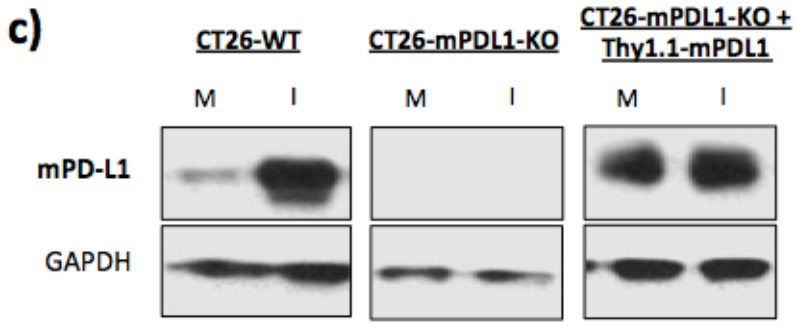
c)
CT26-WT
CT26-mPDL1-KO
CT26-mPDL1-KO + Thy1.1-mPDL1
M
I
M
I
M
I
mPD-L1
GAPDH

Figure 3.7 Validation of mPDL1-expressing cancer cells. (A) Schematic overview of the CFSE EV transfer experimental workflow. (B) CT26-WT, CT26-mPDL1-KO, and CT26-mPDL1-KO + Thy1.1-mPDL1 cells were subjected to flow cytometry to quantify the percentage of single cells positive for mPD-L1 surface expression, out of the total live cell population. The cells were either mock treated, or treated with 50U/well of Recombinant Mouse IFN-γ Protein for 24 hours. Isotype control was included to quantify any non-specific binding from the antibodies. Data represent 2 biological replicates, in which 15000 single, live cells were analyzed. The same cells and conditions were used for (C) Western blot analysis. The membranes were probed for mPD-L1, and GAPDH as a loading control, following mock (M) or 24 hour IFN-γ (I) treatment.

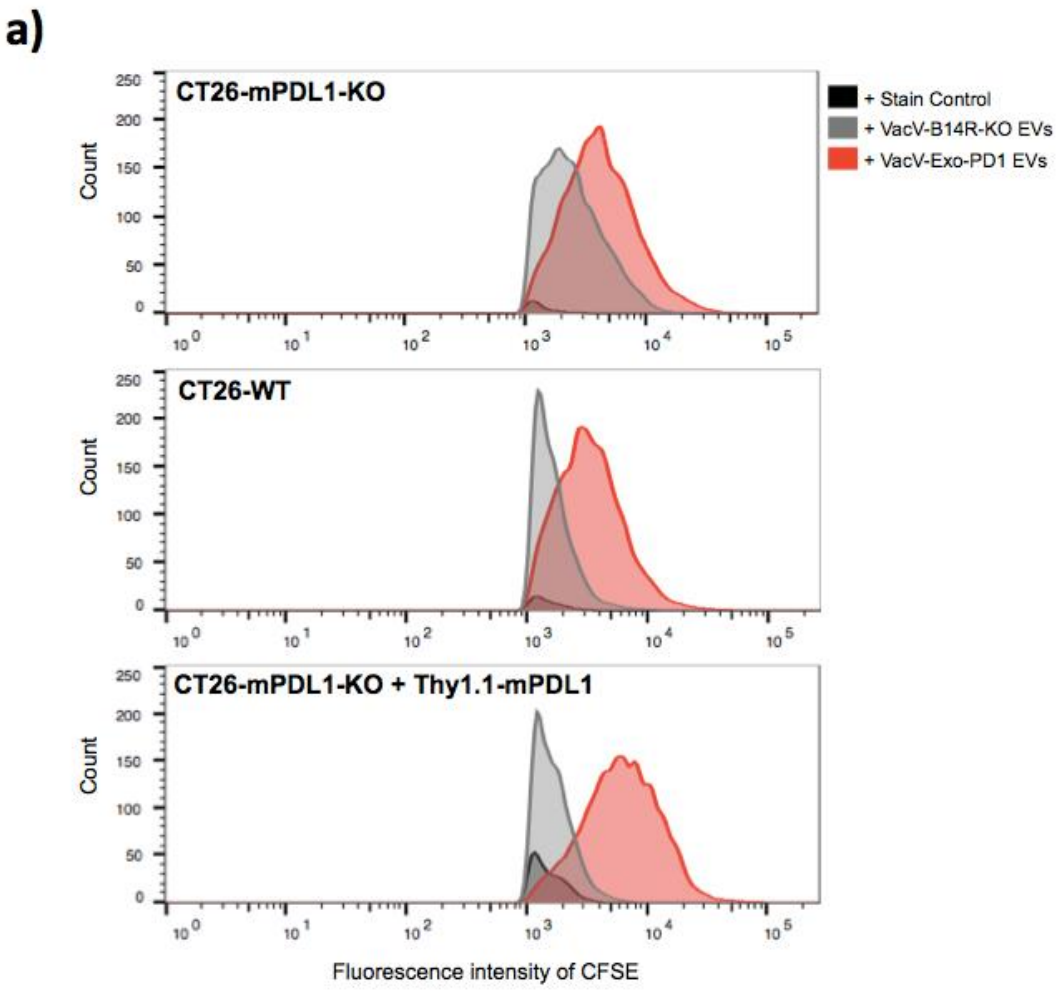

Figure 3.8 EVs displaying the Exo-PD1 chimera are up-taken by mPDL1-expressing cells. Preliminary results using flow cytometry to quantify fluorescence intensity of CFSE following the transfer of CFSE-stained EVs to CT26-WT, CT26-PDL1-KO, or CT26-mPDL1-KO + Thy1.1-mPDL1 cells. EVs were either collected from 786-0 cells 48hpi with VacV-B14R-KO control virus, or VacV-Exo-PD1 virus at an MOI of 1. Prior to transfer, the EVs were analyzed by BCA to normalize the concentration used for each condition. A stain control (with no EVs) was included to quantify non-specific uptake of the CFSE dye alone/background fluorescence signal. Data represent 1 biological replicate, in which 15000 single, live cells were analyzed.

3.4 IC blockade by Exo-PD1 enhances anti-tumour immunity

Once it was confirmed in Section 3.3 that the mPD-1 targeting peptide on the tailored EVs following VacV-Exo-PD1 infection can bind mPD-L1, we sought to investigate our second aim: that the IC blockade exhibited by the EV presentation of mPD1 will also aid in neutralizing the immunosuppressive effects of PD-L1 in the TIME, leading to enhance anti-tumour immunity. To this end, a qPCR-based assay was used to analyze the mRNA levels of characteristic immune markers – IL-2, IFN-γ, TNF-α, and IL-12[121] – of activated T-cells following various EV treatments. In a similar experimental set-up, results reported by Chen *et al.* found that the expression of these immune markers by activated T-cells could be significantly reduced following treatment with PDL1-expressing EVs[121]. To try and reproduce these results, CT26-WT cells were used for collecting EVs, based on their known expression of mPD-L1 (confirmed in Fig 3.7B and 3.7C). For our assay set-up, similar to the one used by Chen *et al.*[121]: T-cells were isolated from mouse spleens; the cells were subjected to overnight activation by anti-CD3e and anti-CD28 antibodies; in parallel, EVs were collected from CT26-WT cells that were either mock-infected, infected with the VacV-B14R-KO control virus, or infected with the VacV-Exo-PD1 virus at an MOI of 10 (a high MOI was used due to the reduced viral infectivity of these cells) for 48 hours; the purified EVs for each condition were then transferred to the activated T-cells, and left for 48 hours; at the end of the 48h EV treatment, RNA was extracted from the T-cells and subjected to qPCR analysis (Fig 3.9A and 3.9B). An additional condition in which no EVs were transferred to the activated T-cells was included (T-cells alone), as well as analysis of TGF-β mRNA levels – this marker functioned as a non-target control, since it is not one of the cytokines known to be altered by EV-induced effects on T-cell function. It is important to mention that prior to

the EV transfer, the EVs for each condition were normalized, such that an equal concentration was used for each condition. We did this so that the concentration of EVs was not a contributing factor in our assay, especially since in Fig 3.1, it was shown that VacV infection leads to increased EV expression, compared to the uninfected (mock) condition. The results from the assay were consistent with Chen *et al.* for the T-cells alone (no EVs), and the mock (mPD-L1^{+} EVs) conditions, exhibiting a loss of immune marker expression following treatment with the mPDL1-expressing EVs, likely owing to the known immunosuppressive effects of mPD-L1[121]. For the VacV-B14R-KO control EVs, there was a restoration of the immune marker expression to a similar level to the control (T-cells alone). For the VacV-Exo-PD1 condition, it was observed that the EVs appeared to have enhanced activating properties due to the significant increase in the expression of the immune markers. We hypothesize that this could be due to the mPD-1 expression, from the Exo-PD1 chimera, being able to neutralize the suppressive effects of mPD-L1 found to be expressed on activated T-cells[138]. However, these results represent initial observations, and additional experiments will need to be performed to follow up. The expression of TGF-β (the non-target control) did not exhibit any significant differences between the tested conditions. Overall, these findings appear to support our working hypothesis that these EVs produced by the VacV-Exo-PD1 virus are functional, and can enhance anti-tumour immune functions.

In order to better characterize the EVs used in this qPCR functionality assay, we took a residual aliquot of the EVs used, and analyzed them by Western blot (Fig 3.10A). The EVs isolated from the mock condition had the greatest level of mPD-L1 expression, when compared to the virus-infected conditions (VacV-B14R-KO and VacV-Exo-PD1); this trend was also observed for the originating WCLs. This reduction in immunosuppressive mPD-L1

expression is likely one of the reasons that the EVs collected from the virus-infected conditions (VacV-B14R-KO control and VacV-Exo-PD1) had enhanced immune-stimulating properties. The EVs were probed for mPD-1, to confirm expression of our EV-targeting chimera, Exo-PD1, for the correct condition. Probing for the EV markers, Alix and CD9[106,134,135], was done in order to confirm equal loading of EVs for each condition. Likewise, the WCLs were additionally probed for loading control, β-actin, and the A27L protein of VacV, to confirm viral infection in the indicated conditions. NTA analysis was also done on these residual EV samples for additional validation that the concentration of EVs added for each condition were equal, and they exhibited similar physical properties (i.e. size distribution; Fig 3.10B).

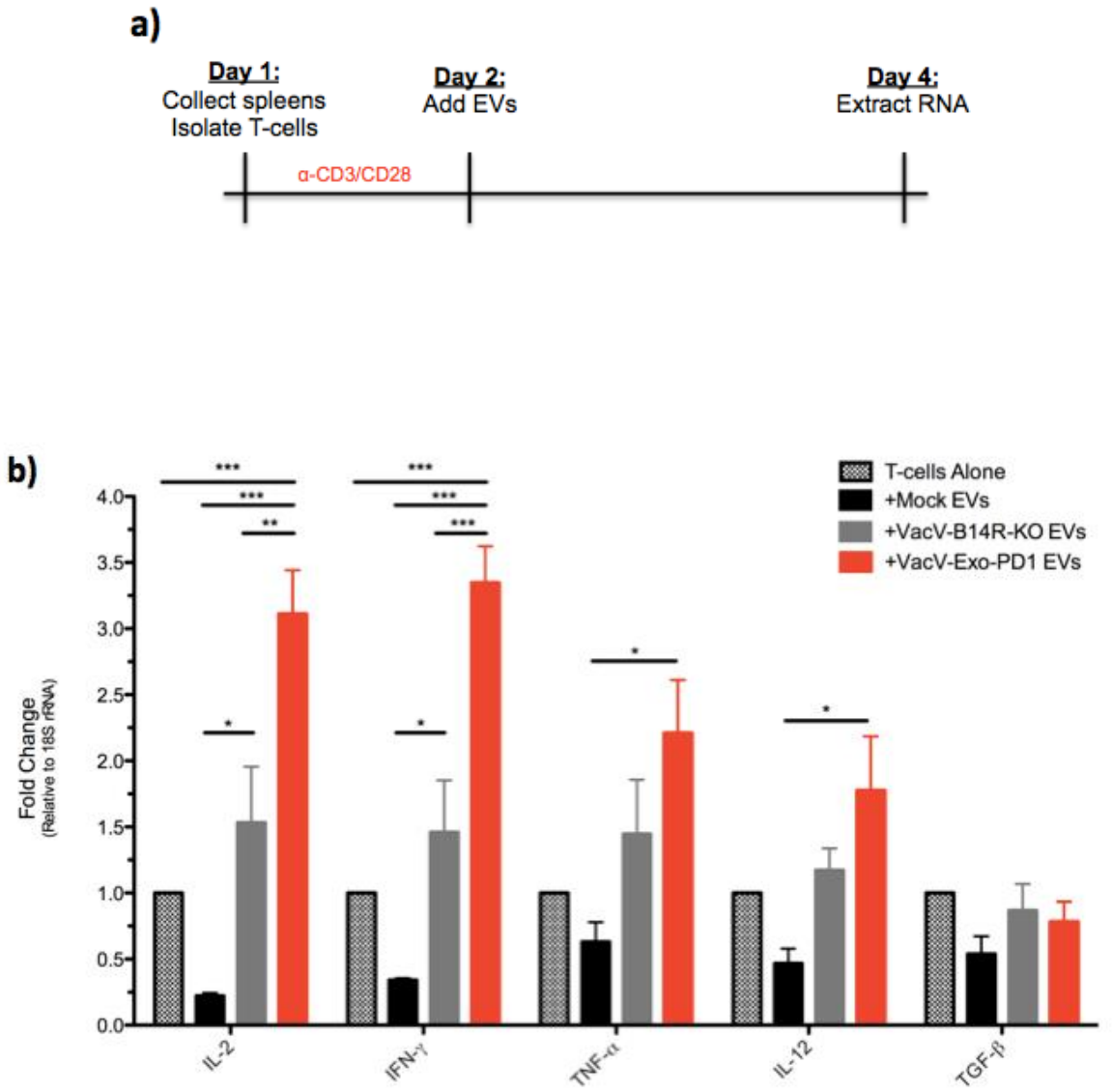

Figure 3.9 EVs produced by VacV-Exo-PD1 infection enhance immune marker expression by T-cells. (A) Schematic of the experimental time-course set-up for the qPCR analysis. (B) qPCR analysis of mRNA collected from murine T-cells following various 48h treatments with normalized concentrations of EVs – EVs were collected from CT26-WT cells: no EVs control (T-cells alone); EVs from mock-infected cells (+Mock EVs); EVs from VacV-B14R-KO control virus-infected cells, MOI 10, 48hpi (+VacV-B14R-KO EVs); and, EVs from VacV-Exo-PD1 virus-infected cells, MOI 10, 48hpi (+VacV-Exo-PD1 EVs). Immune markers: IL-2, IFN-γ, TNF-α, and IL-12[121]. TGF-β was included as a non-target control. Results are plotted as fold change, relative to the 18S rRNA endogenous control. NS: $P>0.05$, *$P<0.05$, **$P<0.01$, ***$P<0.001$ (one-way ANOVA with Tukey's multiple comparison test, for each marker individually) Results represent 2 biological replicates, in which all 4 technical replicates are plotted as independent data points.

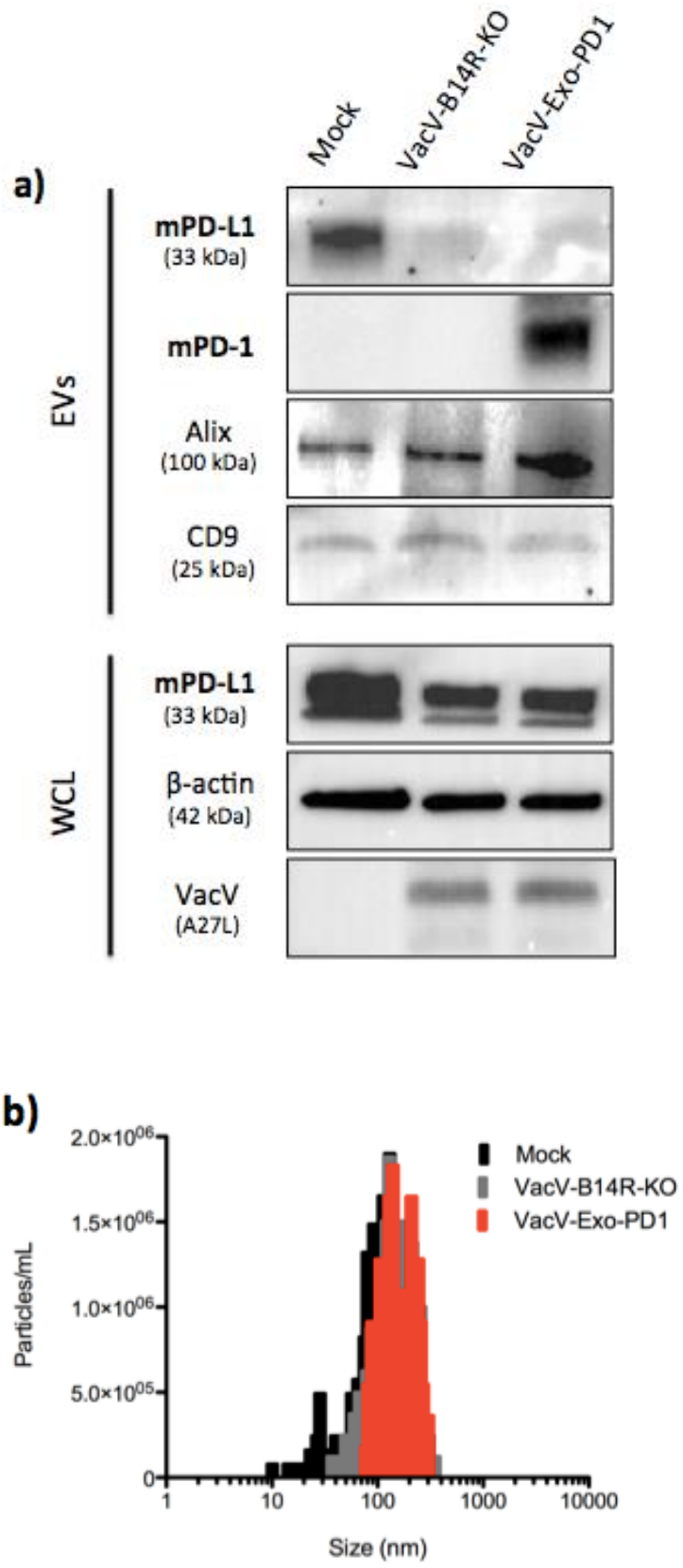
a)
Mock
VacV-B14R-KO
VacV-Exo-PD1
EVs
mPD-L1
(33 kDa)
mPD-1
Alix
(100 kDa)
CD9
(25 kDa)
WCL
mPD-L1
(33 kDa)
β-actin
(42 kDa)
VacV
(A27L)
b)
Particles/mL
2.0×10^06
1.5×10^06
1.0×10^06
5.0×10^05
0
1
10
100
1000
10000
Size (nm)
Mock
VacV-B14R-KO
VacV-Exo-PD1

Figure 3.10 EVs used for immune marker analysis have reduced mPD-L1 expression following VacV infection. A) Western blot analysis of the EVs used in **Fig 3.9**, and their originating WCLs. Membranes were probed for mPD-L1, mPD-1, VacV (A27L protein), EV markers (Alix and CD9), and WCL marker (β-actin). (B) NTA of the same EVs used in **Fig 3.9**.

4. Discussion

4.1 EV expression increases during conditions of stress

Since they were first described back in 1946[139], the study of EVs has garnered major interest, including their role in disease development. While there is still a significant amount of research that needs to be done, their role in response to cellular stress and in the development of cancer resistance has been well studied[140]. In order to promote survival in the TIME, evading cell death and supporting cancer development, cells release EVs as a form of intercellular communication. These signals shared between cells allow adaptation to conditions such as hypoxia or nutrient deprivation, they allow escape from apoptosis and anti-cancer therapies, and they enable immune evasion and disease progression[139–141]. This reaffirms the role that tumour-derived EVs play as key contributors of immunosuppression in the TIME. To further facilitate this cell-to-cell communication during times of stress, EV release is found to increase substantially across a wide range of cell types[142–147]. This led to our initial objective: to demonstrate that following infection with the CopWT strain of VacV, there would be increased expression of EV markers. We theorized that following a viral infection, stressed cancer cells would attempt to send pro-survival signals throughout the TIME via the release of EVs; thereby, resulting in more EVs being released, compared to non-infected cancer cells. Our results from Western blot analysis supported this theory, since greater expression of EV markers was detected following VacV infection of Vero, 786-0, and HT-29 cancer cells, as compared to their non-infected equivalents (Fig 3.1). We were also able to confirm that the EV fractions isolated using our purification method did not test positive for the cellular (non-EV) markers, GM130 (Golgi Apparatus), Calreticulin (Endoplasmic Reticulum), and Tom20 (Mitochondria). This is required for proper

confirmation that the EV isolates are pure, according to the minimal information for the study of extracellular vesicles (MISEV) 2018 guidelines[148]. Probing for the A27L protein of VacV, with no signal detected, also suggests that most viral particles were successfully filtered out of the samples during preparation; future experiments should include additional analysis for the presence of any viral DNA or RNA in the samples for further confirmation. To our knowledge, this is the first time that a connection between VacV infection and increased EV expression has been shown in cancer cells. While these results suggest this trend exists, it is important moving forward that these findings are supplemented with analyses using additional EV characterization methods (ex. NTA, mass spectrometry, etc.). This is especially important when working in the field of EVs, which are known to be a particularly heterogeneous population, to ensure that this trend is consistent across multiple analysis platforms.

4.2 A novel viral technique for generating tailored EVs

The application of EVs for novel therapies has shown great promise, based on their intrinsic abilities to target cells and deliver biological information[112–116]. However, despite all of the advantages associated with using these natural nanoparticle-based vectors[100,125,127–129], obstacles have limited their success in animal models. Currently, the majority of studies using engineered EVs either require the modification of the originating parental cell line, or apply techniques to directly modify the EVs upon purification (ex. by electroporation)[149]. For both cases, this requires methods for large-scale manufacturing of the engineered EVs, and their direct administration, typically by intravenous (IV) delivery. Unfortunately, following IV injection, it has been found that EVs can be cleared from circulation rapidly, before they

are able to exert any therapeutic benefit[150]. Often they are found to accumulate in off-target organs, such as the liver[127]. While this may lead to the proposal that a higher concentration of the EVs should be administered to try and achieve some effect, too high of concentrations can cause aggregation of the EVs in the lungs, and has led to asphyxiation and death in animal models[151]. Therefore, these EV therapies would benefit from a technique that allows targeted delivery in the TIME to avoid normal clearance mechanisms.

In this thesis, we proposed a novel technique in which OVs are engineered to produce tailored EVs *in situ* in the tumour bed. The use of the recombinant OV platform allows selective infection of the cancer cells, which are then induced to release the EVs displaying the engineered chimera. This should allow for their enrichment in the TIME, providing a potential solution to the IV delivery obstacle facing current EV strategies. This technique also complements the previous finding, in which following VacV infection, there was increased expression of EV markers (Fig 3.1). This suggests that a greater number of EVs displaying the engineered construct will be produced locally in the TIME. For our second objective, it was demonstrated that the CopWT strain of VacV could be engineered to produce EVs expressing a targeting peptide of interest, mPD-1 (Fig 3.2). Indeed, following infection with the recombinant VacV-Exo-PD1 virus, expression of mPD-1 was detected for the infected cells and their resulting EVs, and the expression in the supernatant appeared to be concentration-dependent (Fig 3.4A and Fig 3.4B). No signal was detected for the mock-infected cells, or cells infected with the VacV-B14R-KO control virus equivalent. These recombinant viruses, VacV-Exo-PD1 and VacV-B14R-KO control, were also able to result in increased EV marker expression following VacV infection, which is consistent with the findings for the CopWT backbone virus (Fig 3.1). It was also shown that the replication and

growth of the recombinant viruses were not significantly altered by their expression of the transgene constructs (Fig 3.3). This was expected, as we did not anticipate the preferential production of tailored EVs to alter the viral performance. In the future, additional experiments monitoring cell viability should be included as an alternative read-out for monitoring differences in viral infection by recombinant viruses.

In order to exhibit proper tumour cell-targeting abilities, the tailored EVs had to be tested for the correct membrane topology of the Exo-PD1 chimera. For this, an IP pull-down assay was used, and it demonstrated that only EVs collected following VacV-Exo-PD1 infection could be bound by anti-mPD1 antibodies. No EV signal was detected for the mock (non-infected) or VacV-B14R-KO control virus conditions (Fig 3.5). As another control to confirm that this binding and subsequent EV signal for the VacV-Exo-PD1 condition was due to the mPD-1 targeting peptide of the Exo-PD1 chimera, we included a condition in which a negative control anti-IgG antibody was used. As expected, the antibody did not bind to the EVs displaying Exo-PD1, and the EV signal was lost. Overall, these findings demonstrated the successful engineering of a recombinant CopWT virus that produces mPD-1-expressing EVs, suggesting this viral technique is a viable treatment strategy for future EV-based immunotherapies.

4.3 Validation of mPD-1 as a tumour-targeting peptide for EVs

It has been well characterized that PD-L1 plays a key role in establishing immunosuppression in the TIME[50,65]. Therefore, through both innate[66,67] and adaptive[68–70] resistance mechanisms, some tumour cells will up-regulate their expression of PD-L1, and this expression even extends to the cancer-derived exosomes[121–123]. This has led to the

development and success of ICIs targeting the PD-1/PD-L1 axis[71,72]; however, some limitations still exist. In particular, while ICIs targeting PD-1 and PD-L1 are less immunotoxic than anti-CTLA-4 antibodies[50], they still have some undesired effects. It is likely that these therapies could benefit from presentation on a platform such as EVs, based on their natural origin and intrinsic targeting potential. This provided the rationale for adopting our novel viral technique to generate EVs tailored to the tumour target, PD-L1.

Since it was already shown that the Exo-PD1 chimera was being displayed by EVs following VacV-Exo-PD1 infection (Fig 3.4), and with the correct membrane topology (Fig 3.5), we sought to investigate its PD-L1 binding capacity. The initial binding ELISA set-up was used to demonstrate that the mPD-1 targeting peptide of the Exo-PD1 chimera could bind mPD-L1 (Fig 3.6A). Due to technical limitations with the assay, purified EVs alone could not be used to obtain noticeable differences between the binding conditions. It is possible that this is due to the assay requiring additional optimization, and could be explored in future experiments. Instead, cell lysates were used, as they produced the most interpretable and reproducible results. The VacV-Exo-PD1 condition resulted in the greatest fluorescence signal compared to the mock and VacV-B14R-KO control conditions, suggesting that the mPD-1 displayed binds to the mPD-L1 (Fig 3.6B). To confirm that the fluorescence signal observed was not due to non-specific binding, conditions were included in which each sample type was pre-incubated with an anti-mPD-1 antibody, before being added to the binding ELISA set-up. Following this pre-treatment condition, the fluorescence signal initially observed for the VacV-Exo-PD1 lysates was significantly reduced. On the contrary, there was no significant change in fluorescence signal after the anti-mPD-1 pre-treatment for

the mock and VacV-B14R-KO conditions. This further suggested that the signal observed for the VacV-Exo-PD1 condition was in fact, due to the mPD-1 binding to mPD-L1.

Unfortunately, while the binding ELISA is successful at suggesting the binding potential of the mPD-1 peptide for mPD-L1, since purified EVs were not used as input in this assay, I was unable to conclusively confirm the preferential targeting of the EVs for mPD-L1. For this, an additional CFSE EV targeting assay was used based on a successful set-up developed by Chen *et al*[121] (Fig 3.7A). Preliminary results obtained for this CFSE EV transfer assay suggest the targeting potential of the mPD1-expressing EVs. We see that when EVs are collected from 786-0 cells infected with the VacV-Exo-PD1 virus, and transferred to cells with a high level of mPD-L1 expression (CT26-mPDL1-KO + Thy1.1-mPDL1; Fig 3.7B and Fig 3.7C), there is a noticeable shift in fluorescence intensity of CFSE, when compared to the other cell types (CT26-WT and CT26-mPDL1-KO; Fig 3.8). There does not appear to be any differences in fluorescence intensity when the EVs collected from 786-0 cells following VacV-B14R-KO infection are transferred to any of the CT26 cell types. These results suggest a trend of enhanced uptake of EVs displaying the Exo-PD1 targeting chimera by cells with high levels of mPD-L1 expression. Note, the results also closely resemble those observed by Chen *et al*[121]. It is likely that a more significant difference between conditions cannot be observed due to the natural tendency of EVs to be eventually taken up by cells[121,127]. Future studies will benefit from the development of additional assays that can be used to more accurately examine EV-targeting trends.

4.4 Exosomal expression of mPD-L1 is immunosuppressive in the TIME

Exosomal-mPDL1 expression has been recently identified as a key contributor of immunosuppression in the TIME. Its potential as a biomarker has been suggested based on the positive correlation between circulating exosomal-PDL1 levels, with increased tumour size and the presence of pathological features in patients[152–155]. T-cell activation, proliferation, and killing abilities can be restored following the genetic blocking of exosome biogenesis or deletion of *Pd-l1;* however, this effect is immediately halted through the re-introduction of exogenous exosomal PD-L1, highlighting its immunosuppressive potential[123]. It has also been found that, while the exosomal PD-L1 presentation exhibits the same membrane topology and functionality of cell surface PD-L1[121]; contrary to cellular expression, the exosomal presentation is resistant to current anti-PDL1 therapies[123]. As mentioned previously, the explanation for this resistance remains unknown, but this emphasizes the need for a therapy capable of effectively targeting and neutralizing these immunosuppressive nanoparticles. For this project, we hypothesized that using EVs as a platform to deliver and present ICIs in the TIME is one possible strategy, with the potential to promote enhanced anti-tumour immune functions.

4.5 mPD-1 EV presentation can mitigate some immunosuppression

Once it was suggested that the Exo-PD1 chimera was being displayed by EVs following VacV-Exo-PD1 infection (Fig 3.4 and Fig 3.5), and the targeting mPD-1 peptide was binding to mPD-L1 (Fig 3.6 and Fig 3.8), we investigated the functionality of mPD-1 EV presentation in the immune context. For this, qPCR analysis was used to detect the expression of immune markers – IL-2, IFN-γ, TNF-α, and IL-12 – by T-cells following

various EV treatments. To start, our results were consistent with those obtained by Chen *et al*, in which they showed that EVs collected from PDL1-expressing cells had suppressive effects on immune marker expression[121]. This can be seen for the "+Mock EVs" condition, in which EVs were collected from non-infected CT26-WT cells (Fig 3.9). Our results demonstrated that following VacV infection of CT26-WT cells with the control VacV-B14R-KO virus, the immune marker expression could be restored to levels similar to the non-EV treated control ("T-cells alone"). Treatment with the EVs collected following VacV-Exo-PD1 infection led to a significant increase in immune marker expression by the T-cells, supporting our hypothesis that mPD-1 EV presentation enhances anti-tumour immunity. We propose that the most likely explanation for this is that the mPD-1 can neutralize suppressive effects of mPD-L1 found to be expressed on the surface of activated T-cells[138,156]. It is important to note that prior to performing this qPCR assay, we determined the approximate concentration of EVs for each condition. This was done in an effort to add the same concentration of EVs to the T-cells for each condition, such that the results observed were not confounded by this variable. The quantification of TGF-β expression following each EV treatment was included as a non-target control, since its expression is not known to be affected by these EV treatments. Future experiments should include an analysis in which EVs are collected for each condition from the other CT26 cell variants, CT26-mPDL1-KO and CT26-mPDL1-KO + Thy1.1-mPDL1, to determine how the results differ when there are varying levels of mPD-L1 expression. We suspect that for both cell types, there would be a reduction in the significance between EV treatment conditions, since the mPD-L1 levels for the EVs produced should be more consistent across the different conditions (mock, VacV-B14R-KO, and VacV-Exo-PD1). We also propose including an analysis following pre-

treatment with the anti-mPD1 antibody for each condition, similar to what was done for the binding ELISA. This would help to deduce whether the effects on immune marker expression are due to the mPD-1 EV presentation. In addition, since the current working assay was based on a successful set-up by Chen *et al*[121], the T-cells used were activated for 24 hours following isolation, and prior to EV treatment. Therefore, the inhibitory effects that exosomal-mPDL1 expression had on the T-cells was likely more related to inhibiting effector functions, once the T-cells were already activated. We propose including an additional analysis using isolated T-cells without the 24 hour activation, as this will determine if a similar inhibitory effect is observed on T-cell activation.

In an effort to better characterize these EVs, and investigate a possible explanation for why VacV infection led to improved immune marker expression by T-cells following these EV treatments, Western blot analysis (Fig 3.10A) and NTA analysis (Fig 3.10B) were performed. Following VacV infection, the VacV-B14R-KO and VacV-Exo-PD1 conditions displayed reduced EV expression of mPD-L1, which offers a likely explanation for the results seen in Fig 3.9. This trend of reduced mPD-L1 expression following VacV infection was also observed for the originating cell lysates. The EVs were additionally probed for EV markers, Alix and CD9, and analyzed by NTA to ensure that for each treatment, a similar concentration of EVs were used since, as mentioned previously, we did not want this T-cell immune marker analysis to be confounded by additional variables (ex. concentration). Future analyses, such as T-cell killing assays and *in vivo* survival studies, will need to be done to further characterize the functional effects that mPD-1 EV presentation has on anti-tumour immunity. The results from this proof-of-concept project, however, do suggest that this technique of engineering EVs to function as ICIs may be capable of neutralizing

immunosuppression in the TIME more effectively than ICI antibodies, but a direct comparison will need to be performed for confirmation.

4.6 Implications for Exo-PD1 in cancer treatment

The role of EVs following viral infection and in the TIME is starting to be studied, but it remains not well characterized in the context of OVs. We propose a novel technique that combines OVs with an EV-based platform for ICI therapy; thereby, providing the immunostimulation and improved safety profile that these treatments are currently lacking. Throughout this thesis, we demonstrated the ability of using the VacV-Exo-PD1 virus to produce EVs displaying PD-1, to target PDL1-positive cancer cells. We propose that the use of an EV platform for targeted delivery of the immune checkpoint therapy in the TIME will offer advantages over the current antibody-based platform. These advantages, owing to the natural origin of EVs and their role in cell-to-cell communication, include: intrinsic cell-targeting abilities, enhanced biocompatibility and stability, the capacity to transport biological information, and an improved safety profile (compared to other foreign delivery vehicles)[113–116]. We also propose that this EV-based therapy could be used in combination with traditional anti-PDL1 therapies for improved anti-tumour immunity, as the engineered EVs would be able to target and neutralize immunosuppressive EVs in the TIME, while the anti-PDL1 antibodies could target cellular PD-L1 expression. The combination of these two strategies would likely result in the greatest therapeutic benefit. Overall, this thesis serves as a proof-of-concept, paving the way for this novel viral technique to be used for engineering tailored EVs as an immunotherapeutic platform, and the potential experiments that can be performed to characterize the EVs. Future directions will focus on investigating other

potential tumour targeting peptides, and therapeutic cargo that can be loaded in the EVs to further enhance their efficacy.

5. Concluding Remarks

Immunoresistance remains one of the greatest challenges facing cancer treatments today. In this study, we demonstrate the potential of combining the selectivity and immune-stimulating properties of OVs, with EVs as tailored platforms for immune checkpoint blockade. The combination of OVs and ICIs allows us to reap the benefits of each individual therapy, while combatting the limitations that each possessed as a monotherapy. In addition, we propose that engineering EVs for use as an ICI platform will enable targeting of the naturally immunosuppressive EVs in the TIME. Since these EVs are known to be resistant to current ICI therapies, our approach will lead to enhanced anti-tumour immune functions in the TIME. Overall, our work provides insight into a novel therapeutic avenue that can be investigated in hopes of combatting cancer immunoresistance, such that future therapies can target a wider range of cancer models, especially as the number of people affected by cancer continues to rise.

6. References

1. Canadian Cancer Society. Canadian Cancer Society's Advisory Committee on Cancer Statistics. Canadian Cancer Statistics 2017. http://www.cancer.ca/Canadian-Cancer-Statistics-2017-EN.pdf. Published 2017. Accessed June 16, 2019.
2. Gottesman MM, Ludwig J, Xia D, Szakacs G. Defeating Drug Resistance in Cancer. *Discov Med*. 2009;6(31):18-23. http://www.discoverymedicine.com/Michael-M-Gottesman/2009/07/26/defeating-drug-resistance-in-cancer/. Accessed June 17, 2019.
3. Nikolaou M, Pavlopoulou A, Georgakilas AG, Kyrodimos E. The challenge of drug resistance in cancer treatment: a current overview. *Clin Exp Metastasis*. 2018;35(4):309-318. doi:10.1007/s10585-018-9903-0
4. Lichty BD, Breitbach CJ, Stojdl DF, Bell JC. Going viral with cancer immunotherapy. *Nat Rev Cancer*. 2014;14(8):559-567. doi:10.1038/nrc3770
5. Dunn GP, Old LJ, Schreiber RD. The Immunobiology of Cancer Immunosurveillance and Immunoediting. *Immunity*. 2004;21(2):137-148. doi:10.1016/j.immuni.2004.07.017
6. Prendergast GC. Immune escape as a fundamental trait of cancer: focus on IDO. *Oncogene*. 2008;27(28):3889-3900. doi:10.1038/onc.2008.35
7. Wilson RAM, Evans TRJ, Fraser AR, Nibbs RJB. Immune checkpoint inhibitors: new strategies to checkmate cancer. *Clin Exp Immunol*. 2018;191(2):133-148. doi:10.1111/cei.13081
8. Igney FH, Krammer PH. Immune escape of tumors: apoptosis resistance and tumor counterattack. *J Leukoc Biol*. 2002;71(6):907-920. doi:10.1189/jlb.71.6.907
9. Smyth MJ, Swann JB. Immune surveillance of tumors. *J Clin Invest*.

2007;117(5):1137-1146. doi:10.1172/JCI31405

10. Bouzin C, Brouet A, De Vriese J, DeWever J, Feron O. Effects of Vascular Endothelial Growth Factor on the Lymphocyte-Endothelium Interactions: Identification of Caveolin-1 and Nitric Oxide as Control Points of Endothelial Cell Anergy. *J Immunol*. 2007;178(3):1505-1511. doi:10.4049/jimmunol.178.3.1505
11. Buckanovich RJ, Facciabene A, Kim S, et al. Endothelin B receptor mediates the endothelial barrier to T cell homing to tumors and disables immune therapy. *Nat Med*. 2008;14(1):28-36. doi:10.1038/nm1699
12. Oleinika K, Nibbs RJ, Graham GJ, Fraser AR. Suppression, subversion and escape: the role of regulatory T cells in cancer progression. *Clin Exp Immunol*. 2013;171(1):36-45. doi:10.1111/j.1365-2249.2012.04657.x
13. A. F, G.T. M, G. C. T-Regulatory cells: Key players in tumor immune escape and angiogenesis. *Cancer Res*. 2012;72(9):2162-2171. http://cancerres.aacrjournals.org/content/72/9/2162.short. Accessed June 17, 2019.
14. Grivennikov S, Greten F, Cell MK-, 2010 U. Immunity, inflammation, and cancer. *Cell*. 2010;140(6):883-899. https://www.sciencedirect.com/science/article/pii/S0092867410000607. Accessed June 17, 2019.
15. Dong H, Strome S, Salomao D, Medicine HT-N, 2002 U. Tumor-associated B7-H1 promotes T-cell apoptosis: a potential mechanism of immune evasion. *Nat Med*. 2002;8(8):793-800. https://www.nature.com/articles/nm730. Accessed June 17, 2019.
16. Zou W, Chen L. Inhibitory B7-family molecules in the tumour microenvironment. *Nat Rev Immunol*. 2008;8(6):467-477. https://www.nature.com/articles/nri2326. Accessed

June 17, 2019.

17. Postow MA, Chesney J, Pavlick AC, et al. Nivolumab and Ipilimumab versus Ipilimumab in Untreated Melanoma. *N Engl J Med*. 2015;372(21):2006-2017. doi:10.1056/NEJMoa1414428

18. Fesnak AD, June CH, Levine BL. Engineered T cells: The promise and challenges of cancer immunotherapy. *Nat Rev Cancer*. 2016;16(9):566-581. doi:10.1038/nrc.2016.97

19. Jackson H, Rafiq S, Brentjens R. Driving CAR T-cells forward. *Nat Rev Clin Oncol*. 2016;13(6):370-383. https://www.nature.com/nrclinonc/journal/v13/n6/abs/nrclinonc.2016.36.html. Accessed June 24, 2019.

20. Guo C, Manjili M, Subjeck J, Sarkar D, Wang X. Therapeutic cancer vaccines: past, present and future. *Adv Cancer Res*. 2013;119:421-475. doi:10.1016/B978-0-12-407190-2.00007-1.Therapeutic

21. Kaufman HL, Kohlhapp FJ, Zloza A. Oncolytic viruses: a new class of immunotherapy drugs. *Nat Rev Drug Discov*. 2015;14(9):642-662. doi:10.1038/nrd4663

22. Russell SJ, Peng K-W, Bell JC. Oncolytic virotherapy. *Nat Biotechnol*. 2012;30(7):658-670. doi:10.1038/nbt.2287

23. Shmulevitz M, Marcato P, Lee PWK. Unshackling the links between reovirus oncolysis, Ras signaling, translational control and cancer. *Oncogene*. 2005;24(52):7720-7728. doi:10.1038/sj.onc.1209041

24. Dunn GP, Koebel CM, Schreiber RD. Interferons, immunity and cancer

immunoediting. *Nat Rev Immunol*. 2006;6(11):836-848. doi:10.1038/nri1961

25. Chen AT, Samson BL, Crupi MJ, Bell JC. Oncolytic viruses: cytolytic agents, replicating immunotherapeutics or both? *Futur Virol*. 2018;(7):445-448. doi:10.2217/fvl-2018-0047

26. Li X, Wang P, Li H, et al. The Efficacy of Oncolytic Adenovirus Is Mediated by T-cell Responses against Virus and Tumor in Syrian Hamster Model. *Clin Cancer Res*. 2017;23(1):239-249. doi:10.1158/1078-0432.CCR-16-0477

27. Davola ME, Mossman KL. Oncolytic viruses: how "lytic" must they be for therapeutic efficacy? *Oncoimmunology*. 2019;8(6). doi:10.1080/2162402X.2019.1596006

28. Gujar S, Pol JG, Kim Y, Lee PW, Kroemer G. Antitumor Benefits of Antiviral Immunity: An Underappreciated Aspect of Oncolytic Virotherapies. *Trends Immunol*. 2018;39(3):209-221. doi:10.1016/j.it.2017.11.006

29. Andtbacka RHI, Kaufman HL, Collichio F, et al. Talimogene Laherparepvec Improves Durable Response Rate in Patients With Advanced Melanoma. *J Clin Oncol*. 2015;33(25):2780-2788. doi:10.1200/JCO.2014.58.3377

30. Liu BL, Robinson M, Han Z-Q, et al. ICP34.5 deleted herpes simplex virus with enhanced oncolytic, immune stimulating, and anti-tumour properties. *Gene Ther*. 2003;10(4):292-303. doi:10.1038/sj.gt.3301885

31. Twumasi-Boateng K, Pettigrew JL, Kwok YYE, Bell JC, Nelson BH. Oncolytic viruses as engineering platforms for combination immunotherapy. *Nat Rev Cancer*. 2018;18(7):419-432. doi:10.1038/s41568-018-0009-4

32. Guse K, Cerullo V, Hemminki A. Oncolytic vaccinia virus for the treatment of cancer. *Expert Opin Biol Ther*. 2011;11(5):595-608. doi:10.1517/14712598.2011.558838

33. Smith GL, Vanderplasschen A, Law M. *The Formation and Function of Extracellular Enveloped Vaccinia Virus*. Vol 83.; 2002. www.sanger.ac.uk. Accessed June 24, 2019.

34. Guo ZS, Bartlett DL. Vaccinia as a vector for gene delivery. *Expert Opin Biol Ther*. 2004;4(6):901-917. doi:10.1517/14712598.4.6.901

35. Thorne SH. Immunotherapeutic potential of oncolytic vaccinia virus. *Immunol Res*. 2011;50(2-3):286-293. doi:10.1007/s12026-011-8211-4

36. Sivanandam V, Larocca CJ, Chen NG, Fong Y, Warner SG. Oncolytic Viruses and Immune Checkpoint Inhibition: The Best of Both Worlds. 2019. doi:10.1016/j.omto.2019.04.003

37. Sharp DW, Lattime EC. Recombinant Poxvirus and the Tumor Microenvironment: Oncolysis, Immune Regulation and Immunization. *Biomedicines*. 2016;4(3). doi:10.3390/biomedicines4030019

38. Thorne SH, Ho Hwang T, Kirn DH. Vaccinia virus and oncolytic virotherapy of cancer. *Curr Opin Mol Ther*. 2005;7(4).

39. Shen Y, Nemunaitis J. Fighting Cancer with Vaccinia Virus: Teaching New Tricks to an Old Dog. 2004. doi:10.1016/j.ymthe.2004.10.015

40. Merchlinsky M, Moss B. Introduction of foreign DNA into the vaccinia virus genome by in vitro ligation: Recombination-independent selectable cloning vectors. *Virology*. 1992;190(1):522-526. doi:10.1016/0042-6822(92)91246-Q

41. Smith GL, Moss B. Infectious poxvirus vectors have capacity for at least 25 000 base pairs of foreign DNA. *Gene*. 1983;25(1):21-28. doi:10.1016/0378-1119(83)90163-4

42. Puhlmann M, Brown CK, Gnant M, et al. Vaccinia as a vector for tumor-directed gene therapy: biodistribution of a thymidine kinase-deleted mutant. *Cancer Gene Ther*.

2000;7(1):66-73. doi:10.1038/sj.cgt.7700075

43. McCart JA, Ward JM, Lee J, et al. Systemic cancer therapy with a tumor-selective vaccinia virus mutant lacking thymidine kinase and vaccinia growth factor genes. *Cancer Res*. 2001;61(24):8751-8757. http://www.ncbi.nlm.nih.gov/pubmed/11751395. Accessed June 20, 2019.

44. Gnant MFX, Noll LA, Irvine KR, et al. *Tumor-Specific Gene Delivery Using Recombinant Vaccinia Virus in a Rabbit Model of Liver Metastases*. https://academic.oup.com/jnci/article-abstract/91/20/1744/2543860. Accessed June 20, 2019.

45. Peplinski GR, Tsung AK, Casey MJ, et al. In vivo murine tumor gene delivery and expression by systemic recombinant vaccinia virus encoding interleukin-1beta. *Cancer J Sci Am*. 1996;2(1):21-27. http://www.ncbi.nlm.nih.gov/pubmed/9166494. Accessed June 20, 2019.

46. Banaszynski LA, Sellmyer MA, Contag CH, Wandless TJ, Thorne SH. Chemical control of protein stability and function in living mice. *Nat Med*. 2008;14(10):1123-1127. doi:10.1038/nm.1754

47. Torres-Domínguez LE, McFadden G. Poxvirus oncolytic virotherapy. *Expert Opin Biol Ther*. 2019;19(6):561-573. doi:10.1080/14712598.2019.1600669

48. Ferguson MS, Lemoine NR, Wang Y. Systemic Delivery of Oncolytic Viruses: Hopes and Hurdles. *Adv Virol*. 2012;2012:1-14. doi:10.1155/2012/805629

49. Chan WM, McFadden G. Oncolytic Poxviruses. *Annu Rev Virol*. 2014;1(1):191-214. doi:10.1146/annurev-virology-031413-085442

50. Pardoll DM. The blockade of immune checkpoints in cancer immunotherapy. *Nat Rev*

Cancer. 2012. doi:10.1038/nrc3239

51. Schwartz RH. Costimulation of T lymphocytes: the role of CD28, CTLA-4, and B7/BB1 in interleukin-2 production and immunotherapy. *Cell*. 1992;71(7):1065-1068. doi:10.1016/S0092-8674(05)80055-8

52. Lenschow DJ, Walunas TL, Bluestone JA. CD28/B7 SYSTEM OF T CELL COSTIMULATION. *Annu Rev Immunol*. 1996;14(1):233-258. doi:10.1146/annurev.immunol.14.1.233

53. Rudd CE, Taylor A, Schneider H. CD28 and CTLA-4 coreceptor expression and signal transduction. *Immunol Rev*. 2009;229(1):12-26. doi:10.1111/j.1600-065X.2009.00770.x

54. Leach DR, Krummel MF, Allison JP. Enhancement of Antitumor Immunity by. *Science (80-)*. 1988;7(23):1734-1736. http://science.sciencemag.org/content/271/5256/1734.short. Accessed June 17, 2019.

55. Hurwitz AA, Foster BA, Kwon ED, et al. Combination immunotherapy of primary prostate cancer in a transgenic mouse model using CTLA-4 blockade. *Cancer Res*. 2000;60(9):2444-2448. doi:10.1158/0008-5472.can-06-4296

56. Ishida Y, Agata Y, Shibahara K, Honjo T. Induced expression of PD-1, a novel member of the immunoglobulin gene superfamily, upon programmed cell death. *EMBO J*. 1992;11(11):3887-3895. doi:10.1002/j.1460-2075.1992.tb05481.x

57. Kawasaki A, Honjo T, Agata Y, et al. Expression of the PD-1 antigen on the surface of stimulated mouse T and B lymphocytes. *Int Immunol*. 2007;8(5):765-772. doi:10.1093/intimm/8.5.765

58. Keir ME, Butte MJ, Freeman GJ, Sharpe AH. PD-1 and Its Ligands in Tolerance and

Immunity. *Annu Rev Immunol*. 2008;26(1):677-704. doi:10.1146/annurev.immunol.26.021607.090331

59. Yamazaki T, Akiba H, Iwai H, et al. Expression of Programmed Death 1 Ligands by Murine T Cells and APC. *J Immunol*. 2002;169(10):5538-5545. doi:10.4049/jimmunol.169.10.5538

60. McDermott DF, Atkins MB. PD-1 as a potential target in cancer therapy. *Cancer Med*. July 2013:n/a-n/a. doi:10.1002/cam4.106

61. Freeman GJ, Long AJ, Iwai Y, et al. Engagement of the Pd-1 Immunoinhibitory Receptor by a Novel B7 Family Member Leads to Negative Regulation of Lymphocyte Activation. *J Exp Med*. 2000;192(7):1027-1034. doi:10.1084/jem.192.7.1027

62. Dong H, Zhu G, Tamada K, Chen L. B7-H1, a third member of the B7 family, co-stimulates T-cell proliferation and interleukin-10 secretion. *Nat Med*. 1999;5(12):1365-1369. doi:10.1038/70932

63. Latchman Y, Wood CR, Chernova T, et al. PD-L2 is a second ligand for PD-1 and inhibits T cell activation. *Nat Immunol 2001 23*. 2001;2(3):261. doi:10.1038/85330

64. Tseng SY, Otsuji M, Gorski K, et al. B7-DC, a new dendritic cell molecule with potent costimulatory properties for T cells. *J Exp Med*. 2001;193(7):839-846. doi:10.1084/jem.193.7.839

65. Hui E, Su X, Taylor MJ, et al. T cell costimulatory receptor CD28 is a primary target for PD-1-mediated inhibition. *Science (80-)*. 2017;355(6332):1428-1433. doi:10.1126/science.aaf1292

66. Parsa AT, Waldron JS, Panner A, et al. Loss of tumor suppressor PTEN function

increases B7-H1 expression and immunoresistance in glioma. *Nat Med*. 2007;13(1):84-88. doi:10.1038/nm1517

67. Marzec M, Zhang Q, Goradia A, et al. Oncogenic kinase NPM/ALK induces through STAT3 expression of immunosuppressive protein CD274 (PD-L1, B7-H1). *Proc Natl Acad Sci U S A*. 2008;105(52):20852-20857. doi:10.1073/pnas.0810958105

68. Kim J, Myers AC, Chen L, et al. Constitutive and Inducible Expression of B7 Family of Ligands by Human Airway Epithelial Cells. *Am J Respir Cell Mol Biol*. 2005;33(3):280-289. doi:10.1165/rcmb.2004-0129OC

69. Lee S-K, Seo S-H, Kim B-S, et al. IFN-gamma regulates the expression of B7-H1 in dermal fibroblast cells. *J Dermatol Sci*. 2005;40(2):95-103. doi:10.1016/J.JDERMSCI.2005.06.008

70. Wilke CM, Wei S, Wang L, Kryczek I, Kao J, Zou W. Dual biological effects of the cytokines interleukin-10 and interferon-γ. *Cancer Immunol Immunother*. 2011;60(11):1529-1541. doi:10.1007/s00262-011-1104-5

71. Barber DL, Masopust D, Ahmed R, et al. Restoring function in exhausted CD8 T cells during chronic viral infection. *Nature*. 2006;439(7077):682-687. doi:10.1038/nature04444

72. Kamphorst A, Wieland A, Nasti T, Yang S, Zhang R, et al. Rescue of exhausted CD8 T cells by PD-1-targeted therapies is CD28-dependent. *Science*. 2017;355(6332):1423-1427. http://science.sciencemag.org/content/355/6332/1423.abstract. Accessed June 17, 2019.

73. Tivol EA, Borriello F, Schweitzer AN, Lynch WP, Bluestone JA, Sharpe AH. Loss of CTLA-4 leads to massive lymphoproliferation and fatal multiorgan tissue destruction,

revealing a critical negative regulatory role of CTLA-4. *Immunity*. 1995;3(5):541-547. doi:10.1016/1074-7613(95)90125-6

74. Waterhouse P, Zheng Y, Nakamura K, et al. Lymphoproliferative Disorders with Early Lethality in Mice Deficient in Ctla-4. *Science (80-)*. 2011;270(5238):985-988. doi:10.1126/science.1202947

75. Nishimura H, Nose M, Hiai H, Minato N, Honjo T. Development of lupus-like autoimmune diseases by disruption of the PD-1 gene encoding an ITIM motif-carrying immunoreceptor. *Immunity*. 1999;11(2):141-151. doi:10.1016/S1074-7613(00)80089-8

76. Nishimura H, Okazaki T, Tanaka Y, … KN-, 2001 U. Autoimmune dilated cardiomyopathy in PD-1 receptor-deficient mice. *Science (80-)*. 2001;291(5502):319-322. doi:10.1126/science.291.5502.319

77. Zamarin D, Holmgaard RB, Subudhi SK, et al. Localized oncolytic virotherapy overcomes systemic tumor resistance to immune checkpoint blockade immunotherapy. *Sci Transl Med*. 2014;6(226):226ra32. doi:10.1126/scitranslmed.3008095

78. Rajani K, Vile R, Rajani KR, Vile RG. Harnessing the Power of Onco-Immunotherapy with Checkpoint Inhibitors. *Viruses*. 2015;7(11):5889-5901. doi:10.3390/v7112914

79. Callahan MK, Postow MA, Wolchok JD. Targeting T Cell Co-receptors for Cancer Therapy. *Immunity*. 2016;44(5):1069-1078. doi:10.1016/J.IMMUNI.2016.04.023

80. Johnson DB, Peng C, Sosman JA. Nivolumab in melanoma: latest evidence and clinical potential. *Ther Adv Med Oncol*. 2015;7(2):97-106. doi:10.1177/1758834014567469

81. Robert C, Schachter J, Long G V., et al. Pembrolizumab versus Ipilimumab in

Advanced Melanoma. *N Engl J Med*. 2015;372(26):2521-2532. doi:10.1056/NEJMoa1503093

82. Topalian SL, Sznol M, McDermott DF, et al. Survival, durable tumor remission, and long-term safety in patients with advanced melanoma receiving nivolumab. *J Clin Oncol*. 2014;32(10):1020-1030. doi:10.1200/JCO.2013.53.0105

83. Borghaei H, Paz-Ares L, Horn L, et al. Nivolumab versus Docetaxel in Advanced Nonsquamous Non–Small-Cell Lung Cancer. *N Engl J Med*. 2015;373(17):1627-1639. doi:10.1056/NEJMoa1507643

84. Garon EB, Rizvi NA, Hui R, et al. Pembrolizumab for the Treatment of Non–Small-Cell Lung Cancer. *N Engl J Med*. 2015;372(21):2018-2028. doi:10.1056/NEJMoa1501824

85. Larkin J, Chiarion-Sileni V, Gonzalez R, et al. Combined Nivolumab and Ipilimumab or Monotherapy in Untreated Melanoma. *N Engl J Med*. 2015;373(1):23-34. doi:10.1056/NEJMoa1504030

86. Torphy RJ, Zhu Y, Schulick RD. Immunotherapy for pancreatic cancer: Barriers and breakthroughs. *Ann Gastroenterol Surg*. 2018;2(4):274-281. doi:10.1002/ags3.12176

87. Haanen JBAG. Converting Cold into Hot Tumors by Combining Immunotherapies. *Cell*. 2017;170(6):1055-1056. doi:10.1016/J.CELL.2017.08.031

88. Sharma P. The future of immune checkpoint therapy. *Science (80-).* 2014;348(6230):56-51. doi:10.1126/science.aaa8172

89. Gajewski TF. The Next Hurdle in Cancer Immunotherapy: Overcoming the Non–T-Cell–Inflamed Tumor Microenvironment. *Semin Oncol*. 2015;42(4):663-671. doi:10.1053/j.seminoncol.2015.05.011

90. Palucka AK, Coussens LM. The Basis of Oncoimmunology. *Cell*. 2016;164(6):1233-1247. doi:10.1016/J.CELL.2016.01.049

91. Chon HJ, Lee WS, Yang H, et al. Tumor microenvironment remodeling by intratumoral oncolytic vaccinia virus enhances the efficacy of immune checkpoint blockade. *Clin Cancer Res*. 2018;25(5):clincanres.1932.2018. doi:10.1158/1078-0432.CCR-18-1932

92. Martin NT, Bell JC. Oncolytic Virus Combination Therapy: Killing One Bird with Two Stones. *Mol Ther*. 2018. doi:10.1016/j.ymthe.2018.04.001

93. Liu Z, Ravindranathan R, Kalinski P, Guo ZS, Bartlett DL. Rational combination of oncolytic vaccinia virus and PD-L1 blockade works synergistically to enhance therapeutic efficacy. *Nat Commun*. 2017;8(1):14754. doi:10.1038/ncomms14754

94. Du T, Shi G, Li YM, et al. Tumor-specific oncolytic adenoviruses expressing granulocyte macrophage colony-stimulating factor or anti-CTLA4 antibody for the treatment of cancers. *Cancer Gene Ther*. 2014;21(8):340-348. doi:10.1038/cgt.2014.34

95. Engeland CE, Grossardt C, Veinalde R, et al. CTLA-4 and PD-L1 Checkpoint Blockade Enhances Oncolytic Measles Virus Therapy. *Mol Ther*. 2014;22(11):1949-1959. doi:10.1038/MT.2014.160

96. Zamarin D, Holmgaard RB, Ricca J, et al. Intratumoral modulation of the inducible co-stimulator ICOS by recombinant oncolytic virus promotes systemic anti-tumour immunity. *Nat Commun*. 2017;8(1):14340. doi:10.1038/ncomms14340

97. Bartee MY, Dunlap KM, Bartee E. Tumor-Localized Secretion of Soluble PD1 Enhances Oncolytic Virotherapy. *Cancer Res*. 2017;77(11):2952-2963.

doi:10.1158/0008-5472.CAN-16-1638

98. Kleinpeter P, Fend L, Thioudellet C, et al. Vectorization in an oncolytic vaccinia virus of an antibody, a Fab and a scFv against programmed cell death -1 (PD-1) allows their intratumoral delivery and an improved tumor-growth inhibition. *Oncoimmunology*. 2016. doi:10.1080/2162402X.2016.1220467

99. Roy S, Hochberg FH, Jones PS. Extracellular vesicles: the growth as diagnostics and therapeutics; a survey. *J Extracell Vesicles*. 2018;7(1):1438720. doi:10.1080/20013078.2018.1438720

100. EL Andaloussi S, Mäger I, Breakefield XO, Wood MJA. Extracellular vesicles: biology and emerging therapeutic opportunities. *Nat Rev Drug Discov*. 2013;12(5):347-357. doi:10.1038/nrd3978

101. Ellis TN, Kuehn MJ. Virulence and immunomodulatory roles of bacterial outer membrane vesicles. *Microbiol Mol Biol Rev*. 2010;74(1):81-94. doi:10.1128/MMBR.00031-09

102. Gould SJ, Raposo G. As we wait: coping with an imperfect nomenclature for extracellular vesicles. *J Extracell Vesicles*. 2013;2(1):20389. doi:10.3402/jev.v2i0.20389

103. Raposo G, Stoorvogel W. Extracellular vesicles: exosomes, microvesicles, and friends. *J Cell Biol*. 2013;200(4):373-383. doi:10.1083/jcb.201211138

104. Colombo M, Raposo G, Théry C. Biogenesis, Secretion, and Intercellular Interactions of Exosomes and Other Extracellular Vesicles. *Annu Rev Cell Dev Biol*. 2014;30(1):255-289. doi:10.1146/annurev-cellbio-101512-122326

105. Roy S, Lin H-Y, Chou C-Y, et al. Navigating the Landscape of Tumor Extracellular

Vesicle Heterogeneity. *Int J Mol Sci*. 2019;20(6):1349. doi:10.3390/ijms20061349

106. Willms E, Johansson HJ, Mäger I, et al. Cells release subpopulations of exosomes with distinct molecular and biological properties. *Sci Rep*. 2016;6(1):22519. doi:10.1038/srep22519

107. Lee Y, EL Andaloussi S, Wood MJA. Exosomes and microvesicles: extracellular vesicles for genetic information transfer and gene therapy. *Hum Mol Genet*. 2012;21(R1):R125-R134. doi:10.1093/hmg/dds317

108. Al-Nedawi K, Meehan B, Micallef J, et al. Intercellular transfer of the oncogenic receptor EGFRvIII by microvesicles derived from tumour cells. *Nat Cell Biol*. 2008;10(5):619-624. doi:10.1038/ncb1725

109. Lee TH, D'Asti E, Magnus N, Al-Nedawi K, Meehan B, Rak J. Microvesicles as mediators of intercellular communication in cancer—the emerging science of cellular 'debris.' *Semin Immunopathol*. 2011;33(5):455-467. doi:10.1007/s00281-011-0250-3

110. Zomer A, van Rheenen J. Implications of Extracellular Vesicle Transfer on Cellular Heterogeneity in Cancer: What Are the Potential Clinical Ramifications? *Cancer Res*. 2016;76(8):2071-2075. doi:10.1158/0008-5472.CAN-15-2804

111. Fatima F, Nawaz M, Fatima F, Nawaz M. Vesiculated Long Non-Coding RNAs: Offshore Packages Deciphering Trans-Regulation between Cells, Cancer Progression and Resistance to Therapies. *Non-Coding RNA*. 2017;3(1):10. doi:10.3390/ncrna3010010

112. Zhuang X, Xiang X, Grizzle W, et al. Treatment of Brain Inflammatory Diseases by Delivering Exosome Encapsulated Anti-inflammatory Drugs From the Nasal Region to the Brain. *Mol Ther*. 2011;19(10):1769-1779. doi:10.1038/MT.2011.164

113. Pascucci L, Coccè V, Bonomi A, et al. Paclitaxel is incorporated by mesenchymal stromal cells and released in exosomes that inhibit in vitro tumor growth: A new approach for drug delivery. *J Control Release*. 2014;192:262-270. doi:10.1016/J.JCONREL.2014.07.042

114. Sun D, Zhuang X, Xiang X, et al. A Novel Nanoparticle Drug Delivery System: The Anti-inflammatory Activity of Curcumin Is Enhanced When Encapsulated in Exosomes. *Mol Ther*. 2010;18(9):1606-1614. doi:10.1038/MT.2010.105

115. Saari H, Lázaro-Ibáñez E, Viitala T, Vuorimaa-Laukkanen E, Siljander P, Yliperttula M. Microvesicle- and exosome-mediated drug delivery enhances the cytotoxicity of Paclitaxel in autologous prostate cancer cells. *J Control Release*. 2015;220:727-737. doi:10.1016/J.JCONREL.2015.09.031

116. Haney MJ, Klyachko NL, Zhao Y, et al. Exosomes as drug delivery vehicles for Parkinson's disease therapy. *J Control Release*. 2015;207:18-30. doi:10.1016/J.JCONREL.2015.03.033

117. Rak J, Guha A. Extracellular vesicles - vehicles that spread cancer genes. *BioEssays*. 2012;34(6):489-497. doi:10.1002/bies.201100169

118. Peinado H, Alečković M, Lavotshkin S, et al. Melanoma exosomes educate bone marrow progenitor cells toward a pro-metastatic phenotype through MET. *Nat Med*. 2012;18(6):883-891. doi:10.1038/nm.2753

119. Becker A, Thakur BK, Weiss JM, Kim HS, Peinado H, Lyden D. Extracellular Vesicles in Cancer: Cell-to-Cell Mediators of Metastasis. *Cancer Cell*. 2016;30(6):836-848. doi:10.1016/J.CCELL.2016.10.009

120. Peinado H, Zhang H, Matei IR, et al. Pre-metastatic niches: organ-specific homes for

metastases. *Nat Rev Cancer*. 2017;17(5):302-317. doi:10.1038/nrc.2017.6

121. Chen G, Huang A, Zhang W, et al. Exosomal PD-L1 contributes to immunosuppression and is associated with anti-PD-1 response. *nature.com*. https://www.nature.com/articles/s41586-018-0392-8Â . Accessed June 20, 2019.

122. Li I, Nabet BY. Exosomes in the tumor microenvironment as mediators of cancer therapy resistance. *Mol Cancer*. 2019;18(1):32. doi:10.1186/s12943-019-0975-5

123. Poggio M, Hu T, Pai C-C, et al. Suppression of Exosomal PD-L1 Induces Systemic Anti-tumor Immunity and Memory. *Cell*. 2019;177(2):414-427.e13. doi:10.1016/j.cell.2019.02.016

124. Huang AC, Postow MA, Orlowski RJ, et al. T-cell invigoration to tumour burden ratio associated with anti-PD-1 response. *Nature*. 2017;545(7652):60-65. doi:10.1038/nature22079

125. Alvarez-Erviti L, Seow Y, Yin H, Betts C, Lakhal S, Wood MJA. Delivery of siRNA to the mouse brain by systemic injection of targeted exosomes. *Nat Biotechnol*. 2011;29(4):341-345. doi:10.1038/nbt.1807

126. Simhadri VR, Reiners KS, Hansen HP, et al. Dendritic Cells Release HLA-B-Associated Transcript-3 Positive Exosomes to Regulate Natural Killer Function. Zimmer J, ed. *PLoS One*. 2008;3(10):e3377. doi:10.1371/journal.pone.0003377

127. Ohno S, Takanashi M, Sudo K, et al. Systemically injected exosomes targeted to EGFR deliver antitumor microRNA to breast cancer cells. *Mol Ther*. 2013;21(1):185-191. doi:10.1038/mt.2012.180

128. Koh E, Lee EJ, Nam G-H, et al. Exosome-SIRPα, a CD47 blockade increases cancer cell phagocytosis. *Biomaterials*. 2017;121:121-129.

doi:10.1016/j.biomaterials.2017.01.004

129. Seow Y, Wood MJ. Biological Gene Delivery Vehicles: Beyond Viral Vectors. *Mol Ther*. 2009;17(5):767-777. doi:10.1038/MT.2009.41

130. Battaglia M, Pozzi D, Grimaldi S, Parasassi T. Hoechst 33258 staining for detecting mycoplasma contamination in cell cultures: a method for reducing fluorescence photobleaching. *Biotech Histochem*. 1994;69(3):152-156. http://www.ncbi.nlm.nih.gov/pubmed/7520758. Accessed July 3, 2019.

131. Carroll MW, Moss B. *Poxviruses as Expression Vectors*. http://biomednet.com/elecref/0958166900800573. Accessed June 19, 2019.

132. Mooney H, Bernardi G. Introduction of genetically modified organisms into the environment. 1990. http://agris.fao.org/agris-search/search.do?recordID=GB19950016377. Accessed June 27, 2019.

133. Liu T, Shi Y, Du J, et al. Vitamin D treatment attenuates 2,4,6-trinitrobenzene sulphonic acid (TNBS)-induced colitis but not oxazolone-induced colitis. *Sci Rep*. 2016;6(1):32889. doi:10.1038/srep32889

134. Raiborg C, Stenmark H. The ESCRT machinery in endosomal sorting of ubiquitylated membrane proteins. *Nature*. 2009;458(7237):445-452. doi:10.1038/nature07961

135. Kowal J, Tkach M, Théry C. Biogenesis and secretion of exosomes. *Curr Opin Cell Biol*. 2014;29:116-125. doi:10.1016/J.CEB.2014.05.004

136. Stamm CE, Pasko BL, Chaisavaneeyakorn S, et al. Screening Mycobacterium tuberculosis Secreted Proteins Identifies Mpt64 as a Eukaryotic Membrane-Binding Bacterial Effector. *mSphere*. 2019;4(3):e00354-19. doi:10.1128/mSphere.00354-19

137. Monoclonal Antibodies, Proteins, Kits, and Reagents - Leinco Technologies - Leinco

Technologies. https://www.leinco.com/. Accessed July 3, 2019.

138. Tang F, Zheng P. Tumor cells versus host immune cells: whose PD-L1 contributes to PD-1/PD-L1 blockade mediated cancer immunotherapy? *Cell Biosci*. 2018;8:34. doi:10.1186/s13578-018-0232-4

139. Yáñez-Mó M, Siljander PR-M, Andreu Z, et al. Biological properties of extracellular vesicles and their physiological functions. *J Extracell Vesicles*. 2015;4(1):27066. doi:10.3402/jev.v4.27066

140. O'Neill C, Gilligan K, Dwyer R, O'Neill CP, Gilligan KE, Dwyer RM. Role of Extracellular Vesicles (EVs) in Cell Stress Response and Resistance to Cancer Therapy. *Cancers (Basel)*. 2019;11(2):136. doi:10.3390/cancers11020136

141. Maas SLN, Breakefield XO, Weaver AM. Extracellular Vesicles: Unique Intercellular Delivery Vehicles. *Trends Cell Biol*. 2017;27(3):172-188. doi:10.1016/j.tcb.2016.11.003

142. Lv L-H, Wan Y-L, Lin Y, et al. Anticancer drugs cause release of exosomes with heat shock proteins from human hepatocellular carcinoma cells that elicit effective natural killer cell antitumor responses in vitro. *J Biol Chem*. 2012;287(19):15874-15885. doi:10.1074/jbc.M112.340588

143. Wang T, Gilkes DM, Takano N, et al. Hypoxia-inducible factors and RAB22A mediate formation of microvesicles that stimulate breast cancer invasion and metastasis. *Proc Natl Acad Sci U S A*. 2014;111(31):E3234-42. doi:10.1073/pnas.1410041111

144. King HW, Michael MZ, Gleadle JM. Hypoxic enhancement of exosome release by breast cancer cells. *BMC Cancer*. 2012;12(1):421. doi:10.1186/1471-2407-12-421

145. Lehmann BD, Paine MS, Brooks AM, et al. Senescence-Associated Exosome Release from Human Prostate Cancer Cells. *Cancer Res*. 2008;68(19):7864-7871. doi:10.1158/0008-5472.CAN-07-6538

146. Beer L, Zimmermann M, Mitterbauer A, et al. Analysis of the Secretome of Apoptotic Peripheral Blood Mononuclear Cells: Impact of Released Proteins and Exosomes for Tissue Regeneration. *Sci Rep*. 2015;5(1):16662. doi:10.1038/srep16662

147. Xiao X, Yu S, Li S, et al. Exosomes: Decreased Sensitivity of Lung Cancer A549 Cells to Cisplatin. Ahmad A, ed. *PLoS One*. 2014;9(2):e89534. doi:10.1371/journal.pone.0089534

148. Théry C, Witwer KW, Aikawa E, et al. Minimal information for studies of extracellular vesicles 2018 (MISEV2018): a position statement of the International Society for Extracellular Vesicles and update of the MISEV2014 guidelines. *J Extracell Vesicles*. 2018;7(1):1535750. doi:10.1080/20013078.2018.1535750

149. Mentkowski KI, Snitzer JD, Rusnak S, Lang JK. Therapeutic Potential of Engineered Extracellular Vesicles. *AAPS J*. 2018;20(3):50. doi:10.1208/s12248-018-0211-z

150. Revets H, De Baetselier P, Muyldermans S. Nanobodies as novel agents for cancer therapy. *Expert Opin Biol Ther*. 2005;5(1):111-124. doi:10.1517/14712598.5.1.111

151. Smyth T, Kullberg M, Malik N, Smith-Jones P, Graner MW, Anchordoquy TJ. Biodistribution and delivery efficiency of unmodified tumor-derived exosomes. *J Control Release*. 2015;199:145-155. doi:10.1016/J.JCONREL.2014.12.013

152. Zhou J, Mahoney KM, Giobbie-Hurder A, et al. Soluble PD-L1 as a Biomarker in Malignant Melanoma Treated with Checkpoint Blockade. *Cancer Immunol Res*. 2017;5(6):480-492. doi:10.1158/2326-6066.CIR-16-0329

153. Theodoraki M-N, Yerneni SS, Hoffmann TK, Gooding WE, Whiteside TL. Clinical Significance of PD-L1+ Exosomes in Plasma of Head and Neck Cancer Patients. *Clin Cancer Res*. 2018;24(4):896-905. doi:10.1158/1078-0432.CCR-17-2664

154. Ludwig S, Floros T, Theodoraki M-N, et al. Suppression of Lymphocyte Functions by Plasma Exosomes Correlates with Disease Activity in Patients with Head and Neck Cancer. *Clin Cancer Res*. 2017;23(16):4843-4854. doi:10.1158/1078-0432.CCR-16-2819

155. Ricklefs FL, Alayo Q, Krenzlin H, et al. Immune evasion mediated by PD-L1 on glioblastoma-derived extracellular vesicles. *Sci Adv*. 2018;4(3):eaar2766. doi:10.1126/sciadv.aar2766

156. Latchman YE, Liang SC, Wu Y, et al. PD-L1-deficient mice show that PD-L1 on T cells, antigen-presenting cells, and host tissues negatively regulates T cells. *Proc Natl Acad Sci U S A*. 2004;101(29):10691-10696. doi:10.1073/pnas.0307252101

Curriculum Vitae

EDUCATION

Master of Science – Biochemistry 2017 – Present

Dr. John Bell Laboratory, OHRI-University of Ottawa, Ottawa, ON

- Thesis: Characterizing PD-L1-targeting extracellular vesicles produced by oncolytic Vaccinia virus infection
- Recipient of the Ontario Graduate Scholarship (2018-2019; and declined 2017-2018) and the CIHR Frederick Banting and Charles Best Canada Graduate Scholarship-Master's (2017-2018)
- Presented at the International Oncolytic Virus Conference in Oxford, UK and the BioCanRX Summit for Cancer Immunotherapy in Banff, AB
- Successfully completed a bioinformatics workshop on RNA-Seq analysis techniques
- Skills in engineered virus design and cloning techniques, assay development, ELISAs, Flow Cytometry, animal surgery, exosome purification, qPCR, cell culture, bioinformatics analysis

Honours Bachelor of Science – Biochemistry and Biomedical Research Co-op

2012 – 2017

McMaster University, Hamilton, ON

- Recipient of awards, including:
    - NSERC Experience Award in May 2016
    - Dubeck Biochemistry Award (2016-2017) for excellence in research and academics
    - Ross Hume Hall Award (2016-2017) for research excellence, and passion for human and environmental health
    - Ernest Robert MacKenzie Kay Scholarship (2015-2016) for academic excellence
    - Science Class of '97 Legacy Community Contribution Award (2015-2016 and 2016-2017)
- Lab skills in Atomic Force Microscopy (AFM), animal surgery, tissue cultures, Western Blots, Immunocytochemistry, protein purification, CL2 bacterial cultures

PUBLICATIONS

Chen AT, Samson BLR, Crupi MJF, Bell JC (2018). Oncolytic viruses: Cytolytic agents, replicating immunotherapeutics or both? *Future Virology, 13*(7), 445-448, DOI: 10.2217/fvl-2018-0047.

Chen AT and Zou S (2016). Evaluation of drug-mediated arrhythmic changes in spontaneous beating cardiomyocytes by AFM. *Analyst, 141*(22), 6303-6313, DOI: 10.1039/c6an01577h.

Scott A, Wong C, Chen AT, Doering L. Dysregulation of purinergic signaling and alterations in astrocyte physiology in Fragile X Syndrome. *Publication in progress.*

WORK EXPERIENCE

Biology Research Assistant May 2016 – January 2017, May 2017 – September 2017
Research and Development, Spartan Bioscience, Ottawa, ON

- Assisted in developing and optimizing 2 PCR-based assays on different platforms, including the Thermo Fisher QuantStudio 3, Spartan RX, and the Spartan Cube
- Individually designed experiments, and collected either CL-2 level bacterial samples, or collected buccal swab samples in a clean room environment, following GMP and GLP protocols
- Used advanced statistical methods and software for the data processing and interpretation of results
- Worked closely with engineers, sales representatives, and a manufacturing team to develop customer-friendly products for sample collection and analysis
- Participated in inter-departmental meetings to strategize product distribution and marketing

Research Co-op Student January 2015 – September 2015
Department of Measurement Science and Standards, National Research Council of Canada, Ottawa, ON

- Individually performed Atomic Force Microscopy (AFM) imaging and force measurements using a JPK NanoWizard® II to quantify the mechanical properties (beating rates and duration) of human and mouse induced pluripotent stem cell-derived cardiomyocytes (hiPSC-CM, miPSC-CM respectively)
- Attended conferences run by Carleton University and the Canadian Society for Chemistry (CSC) as a representative of the National Research Council, competing in poster competitions
- Used advanced statistical methods and software for the data processing and interpretation of results
- Successfully cultured hiPSC-CMs and miPSC-CMs for living cell AFM analysis
- Assessed numerous therapeutic drug treatments for their effects on the mechanical properties of hiPSC-CM and miPSC-CM cells for contribution towards a publication
- Established an optimized protocol and performed analysis of drug combination therapies based on a self-developed concept, providing a novel approach to the study of cardiomyocyte biology

Research Assistant May 2014 – December 2014
Dr. Laurie Doering Laboratory, McMaster University, Hamilton, ON

- Performed thesis project from September 2015 – May 2016 for 30 hours per week
- Trusted to individually obtain and handle mice of all ages from McMaster's Central Animal Facility following proper Animal Handling and Clean/Vent Room protocols

- Utilized dissecting scope to solely isolate postnatal day 0-6 murine hippocampi or cortices with increased efficiency to reduce potential for contamination
- Assisted in development and performance of optimized Western Blot and Immunocytochemistry protocols to compare P2Y receptor expression and function of murine cortices in wild-type and Fragile X (*Fmr1* gene knock-out) mouse models, for contribution towards a publication
- Successfully generated astrocytes and neurons to analyze co-culturing effects on receptor expression

SKILLS

- Proficient with Microsoft Excel, Word, Office and PowerPoint
- Developing knowledge of French through the Official Languages and Bilingualism Institute
- Sales and marketing skills obtained through previous Retail, Serving and Bartending jobs
- Experienced working with software such as MATLAB, Maple, Origin, IgorPro, Minitab and ImageJ
- Certified in animal handling and surgery for CL-2 and Cleanroom environments through McMaster Central Animal Facility and Animal Care and Veterinary Service at University of Ottawa

EXTRACURRICULAR ACTIVITIES

- Canadian Blood Services volunteer for permanent and mobile clinics since January 2015
- McMaster Children's Hospital arts and crafts volunteer group leader since September 2014
- Biochemistry Department Representative for the McMaster Undergraduate Research in Science Association (MURSA)
- Volunteer representative of the Biochemistry and Biomedical Science Program for "Preview Days"
- Member of the Golden Key International Honours Society awarded for academic achievement (being an undergraduate student in the top 15% of my program)
- "Brotein" mentor for new second year Biochemistry students, providing guidance and wisdom